

# Optimal Stopping via Randomized Neural Networks

**Calypso Herrera**

**Florian Krach**

**Pierre Ruysen**

**Josef Teichmann**

CALYPSO.HERRERA@MATH.ETHZ.CH

FLORIAN.KRACH@MATH.ETHZ.CH

PIERROT@GOOGLE.COM

JOSEF.TEICHMANN@MATH.ETHZ.CH

*Department of Mathematics, ETH Zurich, Rämistrasse 101, 8092 Zurich, Switzerland*

*Google Brain, Google Zurich, Brandschenkestrasse 110, 8002 Zurich, Switzerland*

## Abstract

This paper presents new machine learning approaches to approximate the solution of optimal stopping problems. The key idea of these methods is to use neural networks, where the hidden layers are generated randomly and only the last layer is trained, in order to approximate the continuation value. Our approaches are applicable for high dimensional problems where the existing approaches become increasingly impractical. In addition, since our approaches can be optimized using a simple linear regression, they are very easy to implement and theoretical guarantees can be provided. In Markovian examples our randomized reinforcement learning approach and in non-Markovian examples our randomized recurrent neural network approach outperform the state-of-the-art and other relevant machine learning approaches.

**Keywords:** optimal stopping, least-squares Monte Carlo, reinforcement learning, randomized neural networks, reservoir computing

## 1. Introduction

The optimal stopping problem consists of finding the optimal time to stop in order to maximize an expected reward. This problem is found in areas of statistics, economics, and in financial mathematics. Despite significant advances it remains one of the most challenging problems in optimization, in particular when more than one factor affect the expected reward. A common provable approach widely used is based on Monte Carlo simulations, where the stopping decision is estimated via backward induction (Tsitsiklis and Van Roy, 2001; Longstaff and Schwartz, 2001). Another provable approach is based on reinforcement learning (Bradtke and Barto, 1996; Tsitsiklis and Van Roy, 1997; Yu and Bertsekas, 2007; Li et al., 2009; Chen et al., 2020). Both approaches are based on the ordinary least squares approximation which involves choosing basis functions. While it is simple to choose some set of basis functions, it can be difficult to choose good ones for the considered problem. Moreover, for high dimensions, the number of basis functions often increases polynomially or even exponentially (Longstaff and Schwartz, 2001, Section 2.2), making those algorithms impractical.

A relatively new approach consists of replacing the basis functions by a neural network and performing a gradient descent instead of ordinary least squares (Kohler et al., 2010; Lapeyre and Lelong, 2019; Becker et al., 2019, 2020). The big advantage is that the basis functions do not need to be chosen but are learned instead. Moreover, by its nature, the neural network overcomes the curse of dimensionality, which means that it can easily scale to

high dimensions. However, as the neural network is a non convex function with respect to its parameters, the gradient descent does not necessarily converge to the global minimum, while this is the case for the ordinary least squares minimization. Hence, the main disadvantage of those methods is that there is no convergence guarantees without strong and unrealistic assumptions.

In this paper, we propose two neural network based algorithms to solve the optimal stopping problem for Markovian settings: a backward induction and a reinforcement learning approach. The idea is inspired by randomized neural networks (Cao et al., 2018; Huang et al., 2006). Instead of learning the parameters of all layers of the neural network, the hidden layers are randomly chosen and fixed and only the parameters of the last layer are learned. Hence, the non-convex optimization problem is reduced to a convex problem, that can be solved with linear regression. The hidden layers form random feature maps, which can be interpreted as random basis functions. In particular, in this paper we show that there is actually no need of complicated or a large number of basis functions. In addition, we provide a randomized recurrent neural network approach for non-Markovian settings. We compare our algorithms to the most relevant baselines in terms of accuracy and computational speed in different option pricing problems. With only a fraction of trainable parameters compared to existing methods, we achieve high quality results considerably faster.

## 2. Optimal Stopping via Randomized Neural Networks

One of the most popular and most studied application of optimal stopping is the financial derivative called American option. Hence, we explain our approach in this context.

### 2.1 American Options

An American option gives the holder the right but not the obligation to exercise the option associated with a non-negative payoff function  $g$  at any time up to the maturity. The American option can reasonably be approximated by a Bermudan option, which can be exercised only at some specific dates  $t_0 < t_1 < t_2 < \dots < t_N$ . For equidistant dates we simply write  $0, 1, 2, \dots, N$ .

### 2.2 Option Price and Optimal Stopping.

We assume to have a  $d$ -dimensional Markovian stochastic process  $(X_t)_{t \geq 0}$  describing the stock prices. With respect to a fixed (pricing) probability measure  $\mathbb{Q}$ , the (superhedging seller's) price of the discretized American option can be expressed through the Snell envelope as described by

$$\begin{aligned} U_N &:= g(X_N), \\ U_n &:= \max(g(X_n), \mathbb{E}[\alpha U_{n+1} | X_n]), \quad 0 \leq n < N, \end{aligned} \tag{1}$$

where  $\alpha$  is the step-wise discounting factor. Then the (superhedging seller's) price of the option at time  $n$  is given by  $U_n$  and can equivalently be expressed as the optimal stopping problem

$$U_n = \sup_{\tau \in \mathcal{T}_n} \mathbb{E}[\alpha^{\tau-n} g(X_\tau) | X_n], \tag{2}$$

where  $\mathcal{T}_n$  is the set of all stopping times  $\tau \geq n$ . The smallest optimal stopping time is given by

$$\begin{aligned} \tau_N &:= N, \\ \tau_n &:= \begin{cases} n, & \text{if } g(X_n) \geq \mathbb{E}[\alpha U_{n+1} | X_n], \\ \tau_{n+1}, & \text{otherwise.} \end{cases} \end{aligned} \tag{3}$$

In particular, at maturity  $N$ , the holder receives the final payoff, and the value of the option  $U_N$  is equal to the payoff  $g(X_N)$ . At each time previous to the maturity, the holder decides whether to exercise or not, depending on whether the current payoff  $g(X_n)$  is bigger than the continuation value  $c_n(X_n) := \mathbb{E}[\alpha U_{n+1} | X_n]$ . Combining expression (1), (2) and (3) we can write the price at initial time as

$$U_0 = \max(g(X_0), \mathbb{E}[\alpha^{\tau_1} g(X_{\tau_1})]).$$

In the following we approximate the price  $U_0$  and continuation values  $c_n(X_n)$  which are defined theoretically but cannot be computed directly.

### 2.3 Monte Carlo Simulation and Backward Recursion

We assume to have access to a procedure to sample discrete paths of  $X$  under  $\mathbb{Q}$ . A standard example is that  $X$  follows a certain stochastic differential equation (SDE) with known parameters. Therefore, we can sample  $m$  realizations of the stock paths, where the  $i$ -th realization is denoted by  $x_0, x_1^i, x_2^i, \dots, x_N^i$ , with the fixed initial price  $x_0$ . For each realization, the cash flow realized by the holder when following the stopping strategy (3) is given by the backward recursion

$$\begin{aligned} p_N^i &:= g(x_N^i), \\ p_n^i &:= \begin{cases} g(x_n^i), & \text{if } g(x_n^i) \geq c_n(x_n^i), \\ \alpha p_{n+1}^i, & \text{otherwise.} \end{cases} \end{aligned}$$

As  $p_1^i$  are samples of  $\alpha^{\tau_1-1} g(X_{\tau_1})$ , by the strong law of large numbers we have that almost surely

$$U_0 = \max\left(g(X_0), \lim_{m \rightarrow \infty} \frac{1}{m} \sum_{i=1}^m \alpha p_1^i\right). \tag{4}$$

### 2.4 Randomized Neural Network Approximation of the Continuation Value

For each path  $i$  in  $\{1, 2, \dots, m\}$  and each date  $n$  in  $\{1, 2, \dots, N-1\}$ , the continuation value is  $c_n(x_n^i) = \mathbb{E}[\alpha U_{n+1} | X_n = x_n^i]$ , where  $c_n : \mathbb{R}^d \rightarrow \mathbb{R}$  describes the expected value of the discounted price  $\alpha U_{n+1}$  if we keep the option until next exercising date  $n+1$ , knowing the current value of the stock  $X_n$ . We approximate this continuation value function by a neural network, where only the parameters of the last layer are learned, called randomized neural network. Even though the architecture of the neural network can be general, we present our algorithm with a simple dense shallow neural network, where the extension to deep networks is immediate. We call  $\sigma : \mathbb{R} \rightarrow \mathbb{R}$  the activation function. A common choice is

$\sigma(x) = \tanh(x)$ , however, there are many other suitable alternatives. For any  $d > 0$ , we define  $\sigma : \mathbb{R}^d \rightarrow \mathbb{R}^d$ ,  $\sigma(x) = (\sigma(x_1), \dots, \sigma(x_d))^\top$  for  $x \in \mathbb{R}^d$ . Let  $\vartheta := (A, b) \in \mathbb{R}^{(K-1) \times d} \times \mathbb{R}^{K-1}$  be the parameters of the hidden layer which are randomly and identically sampled and not optimized. In general,  $A$  and  $b$  can be sampled from different distributions that are continuous and cover all of  $\mathbb{R}$ . The distributions and their parameters are hyperparameters of the randomized neural network that can be tuned. For simplicity we use a standard Gaussian distribution. Let us define

$$\phi : \mathbb{R}^d \rightarrow \mathbb{R}^K, x \mapsto \phi(x) = (\sigma(Ax + b)^\top, 1)^\top.$$

and let  $\theta_n := ((A_n)^\top, b_n) \in \mathbb{R}^{K-1} \times \mathbb{R}$  be the parameters that are optimized. Then for each  $n$  the continuation value is approximated by

$$c_{\theta_n}(x) := \theta_n^\top \phi(x) = A_n^\top \sigma(Ax + b) + b_n.$$

## 2.5 Least Squares Optimization of Last Layer's Parameters $\theta_n$

While the parameters  $\vartheta$  of the hidden layer are randomly set, the parameters  $\theta_n$  of the last layer are found by minimizing the squared error of the difference between conditional expectation of the discounted future price and the approximation function. This is equivalent to finding  $\theta_n$  which minimizes  $\mathbb{E}_{\mathbb{Q}}[(c_{\theta_n}(x_n^i, n) - \alpha U_{n+1})^2 | X_n = x_n^i]$  for each date  $n$  in  $\{1, 2, \dots, n-1\}$ . The backward recursive Monte Carlo approximating of this expectation at time  $n$  yields the loss function

$$\psi_n(\theta_n) = \sum_{i=1}^m (c_{\theta_n}(x_n^i) - \alpha p_{n+1}^i)^2. \quad (5)$$

As the approximation function  $c_{\theta_n}$  is linear in the parameters  $\theta_n$ , the minimizer can be found by ordinary least squares. It can be expressed by the following closed form, which is well defined under standard assumptions (see Theorems 6 and 7)

$$\theta_n = \alpha \left( \sum_{i=1}^m \phi(x_n^i) \phi^\top(x_n^i) \right)^{-1} \cdot \left( \sum_{i=1}^m \phi(x_n^i) p_{n+1}^i \right).$$

## 2.6 Splitting the Data Set into Training and Evaluation Set

The parameters  $\theta_n$  are determined using 50% of the sampled paths (training data). Given  $\theta_n$ , the remaining 50% of the sampled paths (evaluation data) are used to compute the option price. By definition, the continuation value  $c_n$  is a conditional expectation, which is not allowed to depend on the future values  $X_{n+1}$ . If the data set was not split, this might not be satisfied, since the loss function (5) uses the future values  $X_{n+1}$ . In particular, the neural network can suffer from overfitting to the training data, by memorizing the paths, instead of learning the continuation value. Our approach is similar to double learning for overcoming the maximization bias (Sutton and Barto, 2018, Section 6.7).

## 2.7 Algorithm

We first sample  $2m$  paths and then proceed backwards as follows. At maturity, the pathwise option price approximation is equal to the payoff, which means that  $p_N^i = g(x_N^i)$ . For each

date  $n$  in  $\{N-1, N-2, \dots, 0\}$ , we first determine  $\theta_n$  as described before using the paths  $\{1, 2, \dots, m\}$ . For all paths  $i \in \{1, 2, \dots, 2m\}$  we then compare the exercise value  $g(x_n^i)$  to the continuation value  $c_{\theta_n}(x_n^i)$  and determine the path-wise option price approximation at time  $n < N$  as

$$p_n^i = \underbrace{g(x_n^i)}_{\text{payoff}} \underbrace{\mathbf{1}_{\{g(x_n^i) \geq c_{\theta}(x_n^i)\}}}_{\text{exercise}} + \underbrace{\alpha p_{n+1}^i}_{\text{discounted future price}} \underbrace{\mathbf{1}_{\{g(x_n^i) < c_{\theta}(x_n^i)\}}}_{\text{continue}}.$$

For the first half of the paths  $\{1, 2, \dots, m\}$ ,  $p_n^i$  is used to compute the parameters  $\theta_{n-1}$ . Finally, the second half of the paths  $\{m+1, \dots, 2m\}$  is used to compute the option price approximation  $p_0 = \max(g(x_0), \frac{1}{m} \sum_{i=m+1}^{2m} \alpha p_1^i)$ . We call this algorithm, which is presented in Algorithm 1, randomized least squares Monte Carlo (RLSM).

---

**Algorithm 1** Optimal stopping via randomized least squares Monte Carlo (RLSM)

---

**Input:** discount factor  $\alpha$ , initial value  $x_0$

**Output:** price  $p_0$

**1:** sample a random matrix  $A \in \mathbb{R}^{(K-1) \times d}$  and a random vector  $b \in \mathbb{R}^{K-1}$

**2:** simulate  $2m$  paths of the underlying process  $(x_1^i, \dots, x_N^i)$  for  $i \in \{1, \dots, 2m\}$

**3:** for each path  $i \in \{1, \dots, 2m\}$ , set  $p_N^i = g(x_N^i)$

**4:** for each date  $n \in \{N-1, \dots, 1\}$

**a:** for each path  $i \in \{1, \dots, 2m\}$ , set  $\phi(x_n^i) = (\sigma(Ax_n^i + b)^\top, 1)^\top \in \mathbb{R}^K$

**b:** set  $\theta_n = \alpha \left( \sum_{i=1}^m \phi(x_n^i) \phi(x_n^i)^\top \right)^{-1} \left( \sum_{i=1}^m \phi(x_n^i) p_{n+1}^i \right)$

**c:** for each path  $i \in \{1, \dots, 2m\}$ , set  $p_n^i = g(x_n^i) \mathbf{1}_{g(x_n^i) \geq \theta_n^\top \phi(x_n^i)} + \alpha p_{n+1}^i \mathbf{1}_{g(x_n^i) < \theta_n^\top \phi(x_n^i)}$

**5:** set  $p_0 = \max(g(x_0), \frac{1}{m} \sum_{i=m+1}^{2m} \alpha p_1^i)$

---

## 2.8 Guarantees of Convergence

We present results that guarantee convergence of the price computed with our algorithm to the correct price of the discretized American option. The formal results with precise definitions and proofs are given in Section 7. In contrast to comparable results for neural networks (Lapeyre and Lelong, 2019; Becker et al., 2019, 2020), our results do not need the assumption that the optimal weights are found by some optimization scheme like stochastic gradient descent. Instead, our algorithms imply that the optimal weights are found and used.

**Theorem 1** (informal). *As the number of sampled paths  $m$  and the number of random basis functions  $K$  go to  $\infty$ , the price  $p_0$  computed with Algorithm 1 converges to the correct price of the Bermudan option.*

## 2.9 Possible Extensions

When the set of pricing measures  $\mathcal{Q}$  has more than one element (in case of an incomplete market), the option price is given by  $\sup_{\mathbb{Q} \in \mathcal{Q}} U_0^\mathbb{Q}$ , where  $U^\mathbb{Q}$  is defined as in (1). Assuming that we can sample from a finite subset  $\mathcal{Q}_1 \subset \mathcal{Q}$ , this price can be approximated by first computing the price for each measure in  $\mathcal{Q}_1$  and taking the maximum of them.

For simplicity we assumed that the payoff function only takes the current price as input,

however, all our methods and results stay valid if  $g(X_n)$  is replaced by a non-negative  $\mathcal{F}_n$ -measurable random variable  $Z_n$ , where  $\mathcal{F}_n$  denotes the information available up to time  $n$ .

### 3. Optimal Stopping via Randomized Reinforcement Learning

In order to avoid approximating the continuation value at each single date  $n \in \{1, \dots, N-1\}$  with a different function, as it is done in Section 2, we can directly learn the continuation function which also takes the time as argument. Hence, instead of having a different function  $c_{\theta_n}(x_n^i)$  for each date  $n$ , we learn one function which is used for all dates  $n$ . As previously, we define  $\vartheta := (A, b) \in \mathbb{R}^{(K-1) \times (d+2)} \times \mathbb{R}^{K-1}$  the parameters of the hidden layer which are randomly chosen and not optimized, and  $\phi : \mathbb{R}^{d+2} \rightarrow \mathbb{R}^K$ ,  $\phi(n, x) = (\sigma(A\tilde{x}_n + b)^\top, 1)^\top$ , where  $\tilde{x}_n = (n, N-n, x_n^\top)^\top$ . Let  $\theta \in \mathbb{R}^K$  define the parameters that are optimized, then the continuation value is approximated by

$$c_\theta(n, x) = \theta^\top \phi(n, x).$$

Instead of having a loop backward in time with  $N$  steps, we iteratively improve the approximation  $c_\theta$ . We start with some (random) initial weight  $\theta_0$  and then iteratively improve it by minimizing the difference between the continuation function  $c_{\theta_k}$  and the prices  $p$  computed with the previous weight  $\theta_{k-1}$ . Moreover, differently than in Section 2, we use the continuation value for the decision whether to continue *and* for the approximation of the discounted future price, as in (Tsitsiklis and Van Roy, 2001). This second algorithm can be interpreted as a randomized fitted Q-iteration (RFQI) and is presented in Algorithm 2. It is a very simple type of reinforcement learning, where the agent has only two possible actions and the agent's decision does not influence the transitions. As a reinforcement learning method, it is based on the assumption that the optimization problem can be modeled by a Markov decision process.

---

#### Algorithm 2 Optimal stopping via randomized fitted Q-Iteration (RFQI)

---

**Input:** discount factor  $\alpha$ , initial value  $x_0$

**Output:** price  $p_0$

**1:** sample a random matrix  $A \in \mathbb{R}^{(K-1) \times (d+2)}$  and a random vector  $b \in \mathbb{R}^{K-1}$

**2:** simulate  $2m$  paths of the underlying process  $(x_1^i, \dots, x_N^i)$  for  $i \in \{1, \dots, 2m\}$

**3:** initialize weights  $\theta = 0 \in \mathbb{R}^K$

**4:** for each iteration  $\ell$  until convergence of  $\theta$

**a:** for each path  $i \in \{1, \dots, 2m\}$ ,

**i:** set  $p_N^i = g(x_N^i)$

**ii:** for each date  $n \in \{1, \dots, N-1\}$ ,

set  $\phi(n, x_n^i) = (\sigma(A\tilde{x}_n^i + b), 1) \in \mathbb{R}^K$

set  $p_n^i = \max(g(x_n^i), \phi(n, x_n^i)^\top \theta)$

**b:** set  $\theta = \alpha \left( \sum_{n=1}^N \sum_{i=1}^m \phi(n, x_n^i) \phi(n, x_n^i)^\top \right)^{-1} \cdot \left( \sum_{n=1}^N \sum_{i=1}^m \phi(n, x_n^i) p_{n+1}^i \right) \in \mathbb{R}^K$

**5:** set  $p_0 = \max(g(x_0), \frac{1}{m} \sum_{i=m+1}^{2m} \alpha p_1^i)$

---

### 3.1 Guarantees of Convergence.

We present results that guarantee convergence of the price computed with our algorithm to the correct price of the discretized American option. The formal results with precise definitions and proofs are given in Section 8.

**Theorem 2** (informal). *As the number of iterations  $L$ , the number of sampled paths  $m$  and the number of random basis functions  $K$  go to  $\infty$ , the price  $p_0$  computed with Algorithm 2 converges to the correct price of the Bermudan option.*

## 4. Optimal Stopping via Randomized Recurrent Neural Networks for Non-Markovian Processes

For non-Markovian processes, for each date  $n$ , the continuation function is no longer a function of the last stock price,  $c_n(X_n)$ , but a function depending on the entire history  $c_n(X_0, X_1, \dots, X_{n-1}, X_n)$ . More precisely, the continuation value is now defined by  $c_n := \mathbb{E}[\alpha g(X_{n+1}) | \mathcal{F}_n]$  where  $\mathcal{F}_n$  denotes the information available up to time  $n$ . Therefore, we replace the randomized feed-forward neural network by a randomized recurrent neural network (randomized RNN), which can utilize the entire information of the path up to the current time  $(x_0, x_1, \dots, x_{n-1}, x_n)$ . In particular, we define  $\vartheta := (A_x, A_h, b) \in \mathbb{R}^{(K-1) \times d} \times \mathbb{R}^{(K-1) \times (K-1)} \times \mathbb{R}^{K-1}$ , the parameters of the hidden layer which are randomly sampled and not optimized. However, their distributions and parameters, which don't have to be the same for  $A_x$  and  $A_h$ , are hyperparameters that can be tuned. Here those tuning parameters are more important as they determine the interplay between past and new information. Moreover, we define

$$\phi : \mathbb{R}^d \times \mathbb{R}^K \rightarrow \mathbb{R}^{K+1}, \quad (x, h) \mapsto \phi(x, h) = (\sigma(A_x x + A_h h + b)^\top, 1)^\top$$

and  $\theta_n := ((A_n)^\top, b_n) \in \mathbb{R}^{K-1} \times \mathbb{R}$ , the parameters that are optimized. Then for each  $n$ , the continuation value is approximated by

$$\begin{cases} h_n & = \sigma(A_x x_n + A_h h_{n-1} + b) \\ c_{\theta_n}(h_n) & = A_n^\top h_n + b_n = \theta_n^\top \phi(x_n, h_{n-1}) \end{cases}$$

with  $h_0 = 0$ . We call this algorithm, which is presented in Algorithm 3, randomized recurrent least squares Monte Carlo (RRLSM).

## 5. Related Work

In this section we present the most relevant approaches for the optimal stopping problem: backward induction either with basis functions or with neural networks and reinforcement learning. Moreover, we explain the connection of our algorithms to randomized neural networks and reservoir computing techniques.

### 5.1 Optimal Stopping

Numerous works studied the optimal stopping problem via different approaches. A common approach consists of using a regression based method to estimate the continuation value

---

**Algorithm 3** Optimal stopping via randomized recurrent neural network (RRLSM)

---

**Input:** discount factor  $\alpha$ , initial value  $x_0$

**Output:** price  $p_0$

**1:** sample random matrices  $A_x \in \mathbb{R}^{(K-1) \times d}$ ,  $A_h \in \mathbb{R}^{(K-1) \times (K-1)}$  and a random vector  $b \in \mathbb{R}^{K-1}$

**2:** simulate  $2m$  paths of the underlying process  $(x_1^i, \dots, x_N^i)$  for  $i \in \{1, \dots, 2m\}$

**3:** for each path  $i \in \{1, \dots, 2m\}$ , set  $p_N^i = g(x_N^i)$

**4:** for each date  $n \in \{N-1, \dots, 1\}$

**a:** for each path  $i \in \{1, \dots, 2m\}$ ,

set  $h_n^i = \sigma(A_x x_n^i + A_h h_{n-1}^i + b)$

set  $\phi_n^i = ((h_n^i)^\top, 1)^\top \in \mathbb{R}^K$

**b:** set  $\theta_n = \alpha (\sum_{i=1}^m \phi_n^i (\phi_n^i)^\top)^{-1} (\sum_{i=1}^m \phi_n^i p_{n+1}^i)$

**c:** for each path  $i \in \{1, \dots, 2m\}$ , set  $p_n^i = g(x_n^i) \mathbf{1}_{g(x_n^i) \geq \theta_n^\top \phi_n^i} + \alpha p_{n+1}^i \mathbf{1}_{g(x_n^i) < \theta_n^\top \phi_n^i}$

**5:** set  $p_0 = \max(g(x_0), \frac{1}{m} \sum_{i=m+1}^{2m} \alpha p_1^i)$

---

(Tilley, 1993; Barraquand and Martineau, 1995; Carriere, 1996; Tsitsiklis and Van Roy, 1997, 2001; Longstaff and Schwartz, 2001; Boyle et al., 2003; Broadie and Glasserman, 2004; Kolodko and Schoenmakers, 2004; Egloff et al., 2007; Jain and Oosterlee, 2015), or the optimal stopping boundary (Andersen, 1999; Garcia, 2003). A different approach uses quantization (Bally and Pagès, 2003; Bally et al., 2005). A dual approach was developed and extended in (Rogers, 2002; Haugh and Kogan, 2004; Rogers, 2010). An in depth review of the different methods is given in (Bouchard and Warin, 2012; Pagès, 2018).

### 5.1.1 OPTIMAL STOPPING VIA BACKWARD INDUCTION

Among those approaches, the most popular are the backward induction methods introduced by Tsitsiklis and Van Roy (2001) and Longstaff and Schwartz (2001). Tsitsiklis and Van Roy (2001) use the approximated continuation value to estimate the current price, by using the following backward recursion

$$p_n^i = \max(g(x_n^i), c_{\theta_n}(x_n^i)). \quad (6)$$

Instead, Longstaff and Schwartz (2001) use the continuation value only for the decision to stop or to continue.

$$p_n^i = \begin{cases} g(x_n^i), & \text{if } g(x_n^i) \geq c_{\theta_n}(x_n^i) \\ \alpha p_{n+1}^i, & \text{otherwise.} \end{cases} \quad (7)$$

The second algorithm is more robust, as the approximation is only used for the decision and not for the estimation of the price. Hence, the method proposed by Longstaff and Schwartz (2001) is the most used method in the financial industry and can be considered as the state-of-the-art. In both papers, the approximation  $c_\theta(x_n^i) = \theta^\top \phi(x_n^i)$  is used, where  $\phi = (\phi_1, \dots, \phi_K)$  is a set of  $K$  basis functions and  $\theta \in \mathbb{R}^K$  are the trainable weights. Possible choices for the basis functions proposed in Longstaff and Schwartz (2001) are Laguerre, Hermite, Legendre, Chebyshev, Gegenbauer, and Jacobi polynomials. While they have the advantage to have convergence, both algorithms do not easily scale to high dimensional

problems since the number of basis function usually grows polynomially or even exponentially (Longstaff and Schwartz, 2001, Section 2.2).

### 5.1.2 OPTIMAL STOPPING VIA BACKWARD INDUCTION USING NEURAL NETWORKS.

One solution to overcome those issues was proposed by Kohler et al. (2010), which consists of approximating the continuation value by a neural network

$$f_{\theta}(x_n^i) \approx c_{\theta}(x_n^i).$$

That way, the features are learned contrary to the basis function which must be chosen. While Kohler et al. (2010) use the backward recursion (6) introduced by Tsitsiklis and Van Roy (2001), both Lapeyre and Lelong (2019) and Becker et al. (2020) use the backward recursion (7) suggested by Longstaff and Schwartz (2001). Instead of approximating the continuation value, Becker et al. (2019) suggested to approximate the whole indicator function presented in (7) by a neural network  $f_{\theta_n}(x_n^i) \approx \mathbf{1}_{\{g(x_n^i) \geq c(x_n^i)\}}$ . Therefore the current price can be estimated by

$$p_n^i = g(x_n^i) \underbrace{f_{\theta_n}(x_n^i)}_{\text{stop}} + \alpha p_{n+1}^i \underbrace{(1 - f_{\theta_k}(x_n^i))}_{\text{continue}}.$$

Moreover, instead of minimizing the loss function (5) in order to find a good approximation of the continuation function, Becker et al. (2019) optimize the parameters by directly maximizing the option price  $\psi_n(\theta_n) = \frac{1}{m} \sum_{i=1}^m \alpha p_n^i$ .

All those methods use a stochastic gradient based method to optimize the parameters of the neural networks. They have to find the parameters of  $N - 1$  neural networks (using a different neural network for each date). Since they use stochastic gradient methods with a non-convex loss function they cannot provide theoretical convergence guarantees, without the strong assumption that they find the optimal parameters.

### 5.1.3 OPTIMAL STOPPING VIA REINFORCEMENT LEARNING

By its nature, reinforcement learning is closely related to the dynamic programming principle as shown in (Sutton and Barto, 2018; Bertsekas and Tsitsiklis, 1996). Moreover the optimal stopping problem is well studied as an application of reinforcement learning (Tsitsiklis and Van Roy, 1997, 2001; Yu and Bertsekas, 2007; Li et al., 2009). In all those methods a linear approximator is used (linear combination of basis functions), similar to the LSM method (Longstaff and Schwartz, 2001). If a standard set of basis functions is used that grows polynomially in the dimension then these methods suffer from the curse of dimensionality. In particular, they cannot practically be scaled to high dimensions as can be seen in our numerical results. To the best of our knowledge, our approach constitutes the first time that randomized neural networks are used to approximate the value function in reinforcement learning.

## 5.2 Randomized Neural Networks and Reservoir Computing

In RLSM and RFQI we use a neural network with randomly sampled and fixed hidden layers, where only the last layer is reinitialized and trained at each date  $n \in \{N - 1, \dots, 1\}$ . The

architecture used at each date can be interpreted as a neural network with random weights (NNRW) studied and reviewed in (Cao et al., 2018), where a universality result was provided in (Huang et al., 2006). Randomized neural networks as approximation function were also studied by Gorban et al. (2016).

Randomized recurrent neural networks are an extension of randomized neural networks. A recurrent neural network (RNN) which is generated randomly where only the readout map is trained, is known as reservoir computing. Not only it reduces the computation time, but also outperforms classical fully trained RNNs in many tasks (Schrauwen et al., 2007; Verstraeten et al., 2007; Lukoševičius and Jaeger, 2009; Gallicchio et al., 2017). Similarly as in reservoir computing, in our randomized recurrent neural network algorithm RRLSM the parameters of the hidden layers are randomly sampled and fixed. However, while reservoir computing trains only one readout map which has the same parameters for all dates, we train a different readout map for each single date  $n \in \{N - 1, \dots, 1\}$ . similar to RLSM.

## 6. Experiments

There are numerous ways to empirically evaluate optimal stopping approaches. Therefore, we choose the most studied settings that were considered in the American option pricing literature. In particular, we only consider synthetic data. Applications to real data involves model calibration which is an independent problem and finally results in applying the optimal stopping algorithm to synthetically generated data again.

Besides our algorithms, we also implemented the baselines and provide all of them at <https://github.com/HeKrRuTe/OptStopRandNN>. The evaluation of all the algorithms was done on the same computer, a dedicated machine with 2×Intel Xeon CPU E5-2697 v2 (12 Cores) 2.70GHz and 256 GiB of RAM.

### 6.1 The Markovian Case

First we evaluate RLSM and RFQI in the standard Markovian setting of American option pricing with different stock models and payoff functions.

#### 6.1.1 STOCK MODELS (BLACK-SCHOLES AND HESTON)

We test our algorithm on two multidimensional stochastic models, Black-Scholes and Heston with fixed parameters. For each model we sample  $m = 20'000$  paths on the time interval  $[0, 1]$  using the Euler-scheme with  $N = 10$  equidistant dates.

The Black Scholes model for a max-call option is a widely used example in the literature (Longstaff and Schwartz, 2001; Lapeyre and Lelong, 2019; Becker et al., 2019). The Stochastic Differential Equation (SDE) describing this model is  $dX_t = rX_t dt + \sigma X_t dW_t$  with  $X_0 = x_0$  where  $(W_t)_{t \geq 0}$  is a  $d$ -dimensional Brownian motion. We choose the drift  $r = 2\%$ , the volatility  $\sigma = 20\%$  and the initial stock price  $x_0 \in \{80, 100, 120\}$ .

To increase the complexity, we also compare on the Heston model (Heston, 1993), which is also used in (Lapeyre and Lelong, 2019). The SDE describing this model is  $dX_t = rX_t dt + \sqrt{v_t} X_t dW_t$ ,  $dv_t = -\kappa(v_t - v_\infty) dt + \sigma \sqrt{v_t} dB_t$  with  $X_0 = x_0$  and  $v_0 = \nu_0$ , where  $(W_t)_{t \geq 0}$  and  $(B_t)_{t \geq 0}$  are two  $d$ -dimensional Brownian motions correlated with factor  $\rho$ . We choose the drift  $r = 2\%$ , the volatility of volatility  $\sigma = 20\%$ , the long term variance

$v_\infty = 0.01$  , the mean reversion speed  $\kappa = 2$ , the correlation  $\rho = -30\%$ , the initial stock price  $x_0 = 100$  and the initial variance  $\nu_0 = 0.01$ .

### 6.1.2 PAYOFFS (MAX CALL, GEOMETRIC PUT AND BASKET CALL)

We test our algorithms on three different type of options: the max call, the geometric put and the basket call. First, we consider the max-call option as it is a classical example used in optimal stopping (Lapeyre and Lelong, 2019; Becker et al., 2019). The payoff of a max call option is defined by  $g(x) = (\max(x_1, x_2, \dots, x_d) - K)_+$  for any  $x = (x_1, x_2, \dots, x_d) \in \mathbb{R}^d$ . Moreover, we also consider the geometric put option as used in (Lapeyre and Lelong, 2019). The payoff of the geometric put option is defined by  $g(x) = (K - (\prod_{i=1}^d x_i)^{1/d})_+$ . We also test on a basket call option Hanbali and Linders (2019), where the payoff is given by  $g(x) = (\frac{1}{d} \sum_{i=1}^d x_i - K)_+$ . For all those three payoffs, the strike  $K$  is set to 100.

### 6.1.3 BASELINES (LSM, NLSM, DOS AND FQI)

We compare RLSM and RFQI to three backward induction algorithms and one reinforcement learning approach. First, the state-of-the-art least squares Monte Carlo (LSM) (Longstaff and Schwartz, 2001). Second, the algorithm proposed by Lapeyre and Lelong (2019), where the basis functions are replaced by a deep neural network (NLSM). Third, the deep optimal stopping (DOS) (Becker et al., 2019), where instead of the continuation value the whole indicator function of the stopping decision is approximated by a neural network. And finally, the fitted Q-iteration (FQI) presented as the second algorithm in (Tsitsiklis and Van Roy, 1997). Li et al. (2009) studied and compared two reinforcement learning based methods (FQI and LSPI) to solve the optimal stopping problem. Since FQI always worked better in our experiments, we only show comparisons to this algorithm.

### 6.1.4 CHOICE OF BASIS FUNCTIONS FOR THE BASELINES

There are many possible choices for the set of basis functions. Longstaff and Schwartz (2001) proposed to use the first 3 weighted Laguerre polynomials for LSM and Li et al. (2009) added 3 additional basis functions of the date for FQI. While the size of this set of basis functions scales linearly with the dimension, it does not include any coupling terms. The classical polynomial basis functions up to the second order are the easiest way to include coupling terms in the basis. To deal with the time dependence of FQI, the relative date  $t/T$  and  $1 - t/T$  are added as additional coordinates to the  $d$ -dimensional stock vector. The size of this basis grows quadratically in the dimension  $d$ , i.e. it has  $1 + 2d + d(d - 1)/2$  elements for LSM and for FQI  $d$  is replaced by  $d + 2$ . The results obtained with the classical polynomials up to degree two were better than with the weighted Laguerre polynomials for LSM and FQI, therefore we only present these results in our Tables. For large  $d$  the computations of LSM and FQI did not terminate within a reasonable amount of time (several hours) and therefore were aborted.

### 6.1.5 NO REGULARIZATION FOR LSM AND FQI

While increasing the number of hidden nodes without applying penalization led to overfitting for RLSM and RFQI , this was not observe for LSM and FQI. In particular, for LSM Ridge

regression ( $L^2$ -penalisation) was tested without leading to better results than standard linear regression. Moreover, comparing the results of FQI, RFQI and DOS for growing dimensions shows, that overfitting does not become a problem when more basis functions are used. Therefore, also for FQI standard linear regression was used as suggested by Tsitsiklis and Van Roy (1997).

#### 6.1.6 ARCHITECTURE OF NEURAL NETWORKS

In order to have a fair comparison in terms of accuracy and in terms of computation time, we use the same number of hidden layers and nodes per layer for all the algorithms.

- As we observed that one hidden layer was sufficient to have a good accuracy (an increase of the number of the hidden layers did not lead to a improvement of the accuracy), we use one hidden layer. Therefore, the NLSM, DOS, and all algorithms that we proposed have only one hidden layer.
- We use 20 nodes for the hidden layer. For RFQI the number of nodes is set to the minimum between 20 and the number of stocks for stability reasons.
- Leaky ReLU is used for RLSM and RFQI and tanh for the randomized recurrent neural network RRLSM. For NLSM and DOS, we use the suggested activation functions, Leaky ReLU for NLSM and ReLU and sigmoid for DOS.
- The parameters  $(A, b)$  of the random neural networks of RLSM and RFQI are sampled using a standard normal distribution with mean 0 and standard deviation 1. For the randomized recurrent neural network of RRLSM, we use a standard deviation of 0.0008 for  $A_x$  and 0.11 for  $A_h$ .

#### 6.1.7 RESULTS AND DISCUSSION

All algorithms are run 10 times and the mean and standard deviation (in parenthesis) of the prices respectively the median of the corresponding computation times are reported.

The increase in time from Black Scholes (Table 1) to Heston (Table 2) is due to the more time consuming simulations of the stock paths. The longer the path simulation takes the less relevant the computation time of the core algorithms becomes. In the case of Black Scholes, the simulation time is negligible such that the difference between the core algorithms is well visible. For the geometric put option (Table 3), we do not present dimensions larger than 20, because prices decrease to 0 when increasing the number of stocks.

When increasing the number of exercise dates from 10 in the other experiments to  $N \in \{50, 100\}$  (Table 4), RFQI and DOS achieve very similar prices, with RFQI being considerably faster especially for high dimensions with many time steps. Increasing the number of dates further, the computation time can become a limiting factor for DOS. The results of FQI were not stable, hence they are not shown here.

In all cases RLSM and RFQI are the fastest algorithms. For  $N = 10$  exercise dates, RFQI always achieves the highest prices. Moreover, for high dimensions RLSM outperforms all other existing algorithms. This is impressive, considering that RLSM has much less trainable parameters than DOS and NLSM, since the hidden layer is randomly fixed and reused for all dates. Moreover, RFQI achieves the highest prices, while having considerably less trainable

$d$	$x_0$	price					duration						
		LSM	DOS	NLSM	RLSM	FQI	RFQI	LSM	DOS	NLSM	RLSM	FQI	RFQI
5	80	5.80 (0.06)	5.96 (0.05)	5.86 (0.13)	<b>5.64 (0.05)</b>	6.08 (0.13)	<b>6.07 (0.11)</b>	15s	22s	9s	<b>6s</b>	8s	<b>6s</b>
	100	26.15 (0.16)	26.82 (0.20)	26.35 (0.19)	<b>25.36 (0.16)</b>	26.78 (0.14)	<b>26.68 (0.25)</b>	15s	23s	13s	<b>6s</b>	8s	<b>6s</b>
	120	50.87 (0.13)	51.50 (0.25)	51.00 (0.17)	<b>49.89 (0.29)</b>	51.70 (0.20)	<b>51.67 (0.17)</b>	15s	23s	13s	<b>6s</b>	8s	<b>6s</b>
10	80	9.88 (0.09)	10.29 (0.12)	9.93 (0.19)	<b>9.63 (0.07)</b>	10.40 (0.12)	<b>10.36 (0.10)</b>	30s	23s	9s	<b>6s</b>	12s	<b>7s</b>
	100	35.12 (0.11)	35.82 (0.14)	35.10 (0.25)	<b>34.18 (0.15)</b>	35.92 (0.13)	<b>35.92 (0.11)</b>	30s	23s	12s	<b>6s</b>	12s	<b>7s</b>
	120	61.63 (0.22)	62.64 (0.21)	61.75 (0.21)	<b>60.67 (0.16)</b>	62.72 (0.22)	<b>62.77 (0.13)</b>	30s	23s	12s	<b>6s</b>	14s	<b>7s</b>
50	80	23.03 (0.09)	24.46 (0.11)	22.72 (0.31)	<b>22.85 (0.07)</b>	24.59 (0.13)	<b>24.47 (0.07)</b>	7m59s	27s	12s	<b>7s</b>	5m25s	<b>8s</b>
	100	53.56 (0.09)	55.00 (0.12)	52.45 (0.41)	<b>53.13 (0.11)</b>	55.34 (0.12)	<b>55.08 (0.14)</b>	7m58s	26s	13s	<b>7s</b>	6m 9s	<b>8s</b>
	120	83.90 (0.20)	85.76 (0.12)	83.12 (0.72)	<b>83.36 (0.15)</b>	85.88 (0.13)	<b>85.79 (0.20)</b>	8m 1s	26s	13s	<b>7s</b>	6m22s	<b>8s</b>
100	80	26.16 (0.09)	30.47 (0.16)	27.64 (0.55)	<b>29.13 (0.10)</b>	30.29 (0.09)	<b>30.58 (0.12)</b>	35m39s	31s	13s	<b>8s</b>	1h17m59s	<b>9s</b>
	100	57.89 (0.14)	62.64 (0.25)	59.04 (0.72)	<b>60.93 (0.10)</b>	62.27 (0.21)	<b>62.79 (0.19)</b>	36m59s	31s	14s	<b>8s</b>	1h18m15s	<b>9s</b>
	120	89.00 (0.15)	94.64 (0.22)	90.20 (1.19)	<b>92.65 (0.04)</b>	94.35 (0.14)	<b>94.91 (0.15)</b>	37m 0s	31s	14s	<b>8s</b>	1h16m15s	<b>9s</b>
500	80	-	42.85 (0.14)	39.18 (1.12)	<b>42.90 (0.05)</b>	-	<b>44.03 (0.08)</b>	-	1m25s	27s	<b>14s</b>	-	<b>15s</b>
	100	-	78.10 (0.14)	73.59 (1.11)	<b>78.22 (0.09)</b>	-	<b>79.50 (0.12)</b>	-	1m41s	30s	<b>14s</b>	-	<b>15s</b>
	120	-	113.27 (0.26)	107.55 (1.26)	<b>113.37 (0.12)</b>	-	<b>115.18 (0.17)</b>	-	1m44s	31s	<b>14s</b>	-	<b>15s</b>
1000	80	-	47.91 (0.12)	44.85 (1.07)	<b>48.56 (0.07)</b>	-	<b>49.66 (0.04)</b>	-	2m58s	45s	<b>22s</b>	-	<b>23s</b>
	100	-	84.43 (0.15)	80.68 (1.20)	<b>85.26 (0.08)</b>	-	<b>86.56 (0.11)</b>	-	2m59s	42s	<b>22s</b>	-	<b>23s</b>
	120	-	121.03 (0.12)	116.82 (1.07)	<b>121.88 (0.15)</b>	-	<b>123.36 (0.21)</b>	-	2m58s	42s	<b>22s</b>	-	<b>22s</b>
2000	80	-	51.18 (0.15)	50.71 (0.62)	<b>54.10 (0.08)</b>	-	<b>55.06 (0.07)</b>	-	6m18s	1m10s	<b>38s</b>	-	<b>37s</b>
	100	-	88.53 (0.13)	87.82 (0.79)	<b>92.19 (0.07)</b>	-	<b>93.29 (0.10)</b>	-	6m17s	1m14s	<b>39s</b>	-	<b>38s</b>
	120	-	125.88 (0.21)	125.24 (0.84)	<b>130.21 (0.12)</b>	-	<b>131.53 (0.07)</b>	-	6m 7s	1m11s	<b>38s</b>	-	<b>37s</b>

Table 1: Max call option on Black Scholes for different number of stocks  $d$  and varying initial stock price  $x_0$ . RFQI achieves the highest prices while being the fastest and having considerably less trainable parameters.

$d$	price					duration						
	LSM	DOS	NLSM	RLSM	FQI	RFQI	LSM	DOS	NLSM	RLSM	FQI	RFQI
5	9.81 (0.05)	10.06 (0.09)	9.95 (0.09)	<b>9.49 (0.08)</b>	10.11 (0.07)	<b>10.09 (0.12)</b>	32s	40s	29s	<b>24s</b>	25s	<b>23s</b>
10	13.33 (0.05)	13.70 (0.11)	13.26 (0.14)	<b>12.98 (0.08)</b>	13.75 (0.06)	<b>13.74 (0.07)</b>	48s	42s	32s	<b>25s</b>	32s	<b>25s</b>
50	21.18 (0.04)	21.88 (0.06)	20.15 (0.34)	<b>21.09 (0.03)</b>	22.05 (0.06)	<b>22.02 (0.06)</b>	8m37s	59s	44s	<b>38s</b>	6m43s	<b>39s</b>
100	22.73 (0.07)	25.38 (0.11)	22.75 (0.43)	<b>24.66 (0.07)</b>	25.43 (0.06)	<b>25.56 (0.06)</b>	38m44s	1m17s	1m 1s	<b>55s</b>	1h18m15s	<b>56s</b>
500	-	33.43 (0.10)	30.52 (0.48)	<b>33.19 (0.06)</b>	-	<b>34.04 (0.04)</b>	-	4m18s	3m15s	<b>3m 3s</b>	-	<b>3m 4s</b>
1000	-	36.64 (0.06)	34.67 (0.29)	<b>36.87 (0.05)</b>	-	<b>37.68 (0.07)</b>	-	8m14s	5m55s	<b>5m47s</b>	-	<b>6m 0s</b>
2000	-	39.20 (0.08)	38.37 (0.38)	<b>40.66 (0.06)</b>	-	<b>41.47 (0.06)</b>	-	16m11s	11m15s	<b>10m51s</b>	-	<b>10m41s</b>

Table 2: Max call option on Heston for different number of stocks  $d$ . RFQI achieves the highest prices while being the fastest and having considerably less trainable parameters.

payoff	$d$	price					duration						
		LSM	DOS	NLSM	RLSM	FQI	RFQI	LSM	DOS	NLSM	RLSM	FQI	RFQI
GeometricPut	1	7.08 (0.11)	6.97 (0.08)	7.05 (0.11)	<b>7.06 (0.06)</b>	6.92 (0.13)	<b>6.96 (0.10)</b>	8s	20s	9s	<b>5s</b>	6s	<b>6s</b>
	5	3.35 (0.04)	3.33 (0.03)	3.32 (0.05)	<b>3.29 (0.05)</b>	3.35 (0.05)	<b>3.34 (0.03)</b>	15s	22s	10s	<b>6s</b>	8s	<b>7s</b>
	10	2.38 (0.04)	2.37 (0.02)	2.35 (0.04)	<b>2.35 (0.03)</b>	2.40 (0.03)	<b>2.40 (0.05)</b>	29s	23s	10s	<b>7s</b>	13s	<b>7s</b>
	20	1.67 (0.01)	1.69 (0.03)	1.59 (0.05)	<b>1.64 (0.03)</b>	1.72 (0.02)	<b>1.72 (0.02)</b>	1m24s	23s	10s	<b>7s</b>	38s	<b>8s</b>
BasketCall	5	4.61 (0.08)	4.58 (0.06)	4.44 (0.07)	<b>4.61 (0.05)</b>	4.62 (0.04)	<b>4.65 (0.03)</b>	15s	22s	10s	<b>6s</b>	8s	<b>7s</b>
	10	3.58 (0.03)	3.60 (0.05)	3.38 (0.05)	<b>3.61 (0.05)</b>	3.61 (0.06)	<b>3.63 (0.03)</b>	30s	23s	10s	<b>6s</b>	21s	<b>7s</b>
	50	2.05 (0.03)	2.35 (0.02)	1.66 (0.07)	<b>2.00 (0.02)</b>	2.36 (0.02)	<b>2.37 (0.02)</b>	7m59s	27s	12s	<b>7s</b>	5m40s	<b>8s</b>
	100	1.18 (0.01)	2.11 (0.02)	1.24 (0.04)	<b>1.78 (0.01)</b>	2.10 (0.02)	<b>2.12 (0.02)</b>	40m34s	31s	14s	<b>8s</b>	1h17m19s	<b>9s</b>
	500	-	1.92 (0.01)	0.86 (0.02)	<b>1.71 (0.01)</b>	-	<b>1.95 (0.01)</b>	-	1m33s	30s	<b>15s</b>	-	<b>15s</b>
	1000	-	1.91 (0.01)	0.80 (0.02)	<b>1.77 (0.00)</b>	-	<b>1.95 (0.01)</b>	-	2m56s	48s	<b>22s</b>	-	<b>22s</b>
2000	-	1.85 (0.00)	0.77 (0.01)	<b>1.84 (0.00)</b>	-	<b>1.96 (0.00)</b>	-	5m17s	1m22s	<b>39s</b>	-	<b>37s</b>	

Table 3: Geometric put and basket call options on Black Scholes for different number of stocks  $d$ . RFQI achieves the highest prices while being the fastest and having considerably less trainable parameters.

$d$	$N$	price					duration				
		LSM	DOS	NLSM	RLSM	RFQI	LSM	DOS	NLSM	RLSM	RFQI
10	50	34.54 (0.10)	36.06 (0.16)	35.95 (0.17)	<b>33.13 (0.21)</b>	<b>35.98 (0.14)</b>	2m45s	1m50s	1m 8s	<b>33s</b>	<b>37s</b>
	100	34.36 (0.10)	36.11 (0.14)	35.97 (0.20)	<b>32.75 (0.25)</b>	<b>35.83 (0.15)</b>	5m23s	3m55s	2m20s	<b>1m 7s</b>	<b>1m13s</b>
50	50	53.14 (0.08)	55.87 (0.14)	55.21 (0.21)	<b>52.29 (0.08)</b>	<b>55.64 (0.13)</b>	44m28s	2m 5s	1m15s	<b>37s</b>	<b>44s</b>
	100	52.77 (0.11)	56.08 (0.14)	55.60 (0.13)	<b>51.81 (0.09)</b>	<b>55.66 (0.13)</b>	1h30m27s	4m35s	2m34s	<b>1m14s</b>	<b>1m29s</b>
100	50	-	63.81 (0.14)	62.54 (0.22)	<b>60.42 (0.12)</b>	<b>63.58 (0.13)</b>	-	2m53s	1m25s	<b>42s</b>	<b>48s</b>
	100	-	64.10 (0.12)	63.22 (0.12)	<b>59.92 (0.07)</b>	<b>63.58 (0.07)</b>	-	5m57s	2m50s	<b>1m25s</b>	<b>1m37s</b>
500	50	-	80.86 (0.07)	76.45 (0.62)	<b>78.51 (0.07)</b>	<b>81.11 (0.07)</b>	-	8m50s	2m47s	<b>1m16s</b>	<b>1m20s</b>
	100	-	81.26 (0.11)	78.07 (0.42)	<b>78.15 (0.11)</b>	<b>81.21 (0.10)</b>	-	17m36s	5m37s	<b>2m34s</b>	<b>2m40s</b>

Table 4: Max call option on Black Scholes for different number of stocks  $d$  and higher number of exercise dates  $N$ . RFQI achieves similar prices as DOS while being the fastest and having considerably less trainable parameters.

parameters, since only one neural network (with a random hidden layer) of the respective size is used for all exercise dates. In total, RFQI has 21 trainable parameters, compared to more than  $20dN$  for DOS and NLSM.

Comparing the achieved prices of LSM and FQI, we can confirm the claim of Li et al. (2009), that reinforcement learning techniques outperform the state-of-the-art in the Markovian setting. RFQI achieving similar prices as FQI therefore naturally outperforms RLSM which achieves similar prices as LSM. A possible explanation for the outperformance of the reinforcement learning algorithm is the following. The backward induction algorithms have approximately  $N$  times the number of trainable parameters used in the reinforcement learning algorithms, since a different network is trained for each discretization date. Moreover, for the backward induction algorithms, a different continuation value function is approximated for each date, hence only the data of this date is used to learn the parameters. In contrast, the reinforcement learning methods train their parameters using the data of all dates. Hence, the reinforcement learning methods use  $N$  times the number of data to train  $1/N$  times the number of parameters, which might lead to better approximations.

### 6.1.8 EMPIRICAL CONVERGENCE STUDY

We confirm the theoretical results of Theorem 1 (Figure 1 left) and Theorem 2 (Figure 1 right) by an empirical convergence study for a growing number of paths  $m$ . For RLSM we also grow the number of hidden nodes  $K$ , while they are fixed for RFQI since  $d = 5$  is used. For each combination of the number of paths  $m$  and the hidden size  $K$ , the algorithms are run 20 times and their mean prices with standard deviations are shown. For small  $m$  we see that smaller hidden sizes achieve better prices. This is due to overfitting to the training paths when using larger networks. Regularization techniques like  $L^1$ - or  $L^2$ -penalization could be used to reduce overfitting for larger networks. However our results suggest that restricting the hidden size is actually the simplest and best regularization technique, since it additionally leads to lower training times.

## 6.2 The Non-Markovian Case

In order to compare our algorithms on a stochastic process which is not Markovian, we take the example of the fractional Brownian motion  $(W_t^H)_{t \geq 0}$  as in (Becker et al., 2019).

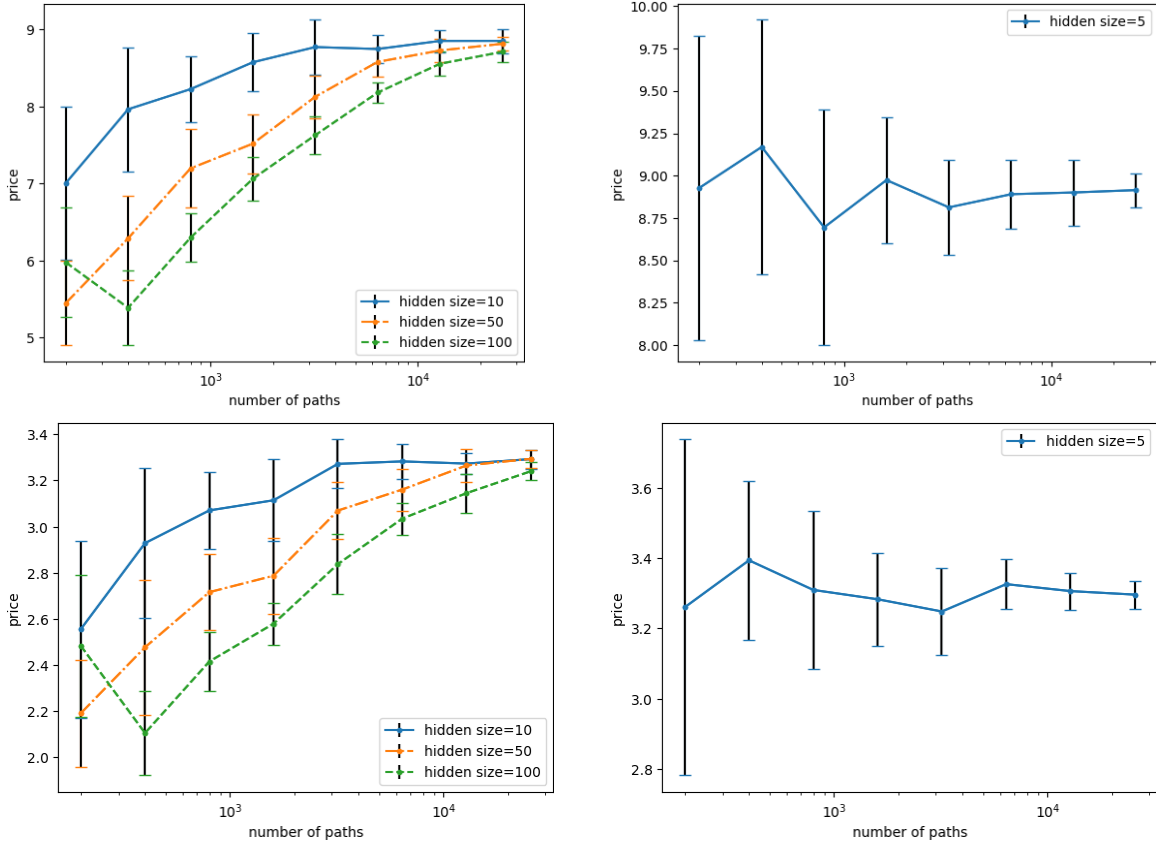


Figure 1: Mean  $\pm$  standard deviation (bars) of the price for a max-call on 5 stocks following the Black Scholes model (up) or the Heston model (down) for RLSM (right) and RFQI (left) for varying the number of paths  $m$  and varying for RLSM the number of neurones in the hidden layer  $K$ .

Unlike classical Brownian motion, the increments of fractional Brownian motion need not be independent. Fractional Brownian motion is a continuous centered Gaussian process with covariation function  $E(W_t^H W_s^H) = \frac{1}{2}(|t|^{2H} + |s|^{2H} + |t-s|^{2H})$  where  $H \in (0, 1)$  is called the Hurst parameter. When the Hurst parameter  $H = 0.5$ , then  $W^H$  is a standard Brownian motion, when  $H \neq 0.5$ , the increments of  $(W_t^H)_{t \geq 0}$  are correlated (positively if  $H > 0.5$  and negatively if  $H < 0.5$ ) which means that for  $H \neq 0.5$ ,  $(W_t^H)_{t \geq 0}$  is not Markovian (Bayer et al., 2016; Livieri et al., 2018; Gatheral et al., 2018; El Euch et al., 2018; Abi Jaber and El Euch, 2019).

### 6.2.1 PAYOFFS AND BASELINES

In the 1-dimensional case we use the identity function as payoff as in (Becker et al., 2019), which can lead to negative values. Moreover, we use the maximum  $g(x) = \max(x_1, x_2, \dots, x_d)$  for any  $x = (x_1, x_2, \dots, x_d) \in \mathbb{R}^d$  and the mean  $g(x) = 1/d \sum_{i=1}^d x_i$  as payoffs for higher dimensions. The initial stock price  $x_0$  is 0. We compare RLSM and RRLSM to DOS and the path-version of DOS (pathDOS), where the entire path until current date is used as input

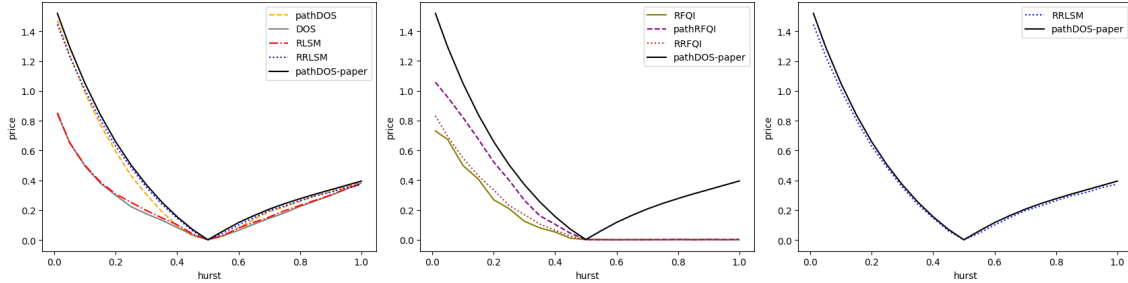


Figure 2: Left: algorithms processing path information outperform. Middle: reinforcement learning algorithms do not work well in non-Markovian case. Right: RRLSM achieves similar results as reported in (Becker et al., 2019), while using only 20K paths instead of 4M for training which took only 4s instead of the reported 430s.

(Becker et al., 2019). Moreover, we test RFQI and its recurrent and path-version in this setting.

### 6.2.2 RESULTS AND DISCUSSION

For  $d = 1$ , we clearly see the outperformance of algorithms processing information of the path compared to the ones using only the current value as input (Figure 2 left). Moreover, this application highlights the limitation of reinforcement learning techniques when applied in non-Markovian settings as discussed in (Kaelbling et al., 1996). In particular, RFQI, the randomized RNN version of it and its path-version do not work well in this example (Figure 2 middle).

RRLSM achieves very similar results as were reported for pathDOS in (Becker et al., 2019), while using only 20K instead of 4M paths (Figure 2 right). At the same time, RRLSM needs only 4s in contrast to 430s reported in their paper. In a different setup, similar to the evaluation of RRLSM, our implementation of pathDOS using the same number of 20 hidden nodes as RRLSM is trained on 20K paths. Then pathDOS takes 154s and achieves worse results than RRLSM (Figure 2 left).

For higher dimensions, we use the small hurst parameter  $H = 0.05$  for which a big difference between the standard and the path dependent algorithms was visible in the 1-dimensional case. RRLSM achieves similar prices as pathDOS for the mean payoff and the highest prices for the max payoff, while considerably outperforming pathDOS in terms of speed (Table 5).

## 7. Convergence of the Randomized Least Square Monte Carlo (RLSM)

We first introduce some technical notation that will be helpful for the proofs. Then we describe the steps from the theoretical idea of RLSM to its implementable version that was presented in Section 2.7. These descriptions are based on (Tsitsiklis and Van Roy, 2001; Clément et al., 2001). We continue by proving a novel universal approximation theorem for randomized neural networks that is used to prove the main result.

payoff	$d$	price				duration			
		DOS	pathDOS	RLSM	<b>RRLSM</b>	DOS	pathDOS	RLSM	<b>RRLSM</b>
Identity	1	0.66 (0.01)	1.24 (0.01)	0.65 (0.02)	<b>1.23 (0.01)</b>	1m15s	2m34s	3s	<b>4s</b>
Max	5	1.72 (0.04)	1.59 (0.01)	2.08 (0.01)	<b>2.15 (0.01)</b>	1m32s	12m55s	15s	<b>15s</b>
	10	1.85 (0.03)	1.68 (0.01)	2.45 (0.00)	<b>2.46 (0.00)</b>	1m47s	26m21s	22s	<b>24s</b>
Mean	5	0.29 (0.00)	0.52 (0.00)	0.28 (0.01)	<b>0.52 (0.01)</b>	1m30s	12m57s	12s	<b>14s</b>
	10	0.20 (0.01)	0.36 (0.00)	0.22 (0.02)	<b>0.32 (0.02)</b>	1m44s	25m19s	28s	<b>21s</b>

Table 5: Identity, maximum and mean on the fractional Brownian motion with  $H = 0.05$  and different number of stocks  $d$ . RRLSM achieves high prices while being much faster than pathDOS.

## 7.1 Definitions

We assume to have a sequence of infinitely many *random* basis functions  $\phi = (\phi_k)_{k \geq 1}$ , where each  $\phi_k$  is of the form

$$\phi_k : \mathbb{R}^d \rightarrow \mathbb{R}, x \mapsto \phi_k(x) := \sigma(\alpha_k^\top x + \beta_k),$$

with  $\sigma$  a bounded activation function,  $\alpha_k \in \mathbb{R}^d$  and  $\beta_k \in \mathbb{R}$ . The parameters  $\alpha_k$  and  $\beta_k$  have i.i.d. entries with a standard Gaussian distribution, hence the name *random* basis functions. With  $(\tilde{\Omega}, \tilde{\mathcal{F}}, \tilde{\mathbb{P}})$  we denote the probability space on which the random weights are defined. For each  $K \in \mathbb{N}$  we define the operator  $\Phi_K$  acting on  $\theta = (\theta_1, \dots, \theta_K) \in \mathbb{R}^K$  by

$$(\Phi_K \theta)(x) := \theta^\top \phi(x) := \sum_{k=1}^K \theta_k \phi_k(x).$$

In particular,  $\Phi_K$  is the operator producing a linear combination of the first  $K$  random basis functions. We assume to have a Markovian discrete time stochastic process  $X = (X_0, \dots, X_N)$  defined on a filtered probability space  $(\Omega, \mathcal{F}, (\mathcal{F}_n)_{n=0}^N, \mathbb{P})$ . In particular, each  $X_n$  is a  $\mathcal{F}_n$ -measurable random variable. We assume that there exists an absolutely continuous measure  $\mathbb{Q} \ll \mathbb{P}$ , the pricing measure, and that the distribution of  $X_n$  under  $\mathbb{Q}$  is  $\pi_n$ . For expectations with respect to these random variables under  $\mathbb{Q}$ , we write  $\mathbb{E}[\cdot]$ . For  $0 \leq n \leq N$  we use the norm

$$\|f\|_{\pi_n}^2 := \mathbb{E}[|f(X_n)|_2^2] = \int_{\mathbb{R}} |f(x)|_2^2 d\pi_n(x),$$

where  $|\cdot|_2$  is the Euclidean norm and  $f$  a measurable function. We introduce the operators  $E_n$  and  $\Pi_n^K$  defined by

$$(E_n J)(x) := \mathbb{E}[J(X_{n+1}) | X_n = x],$$

$$(\Pi_n^K J) := \arg \min_{\Phi_K \theta} \|J - \Phi_K \theta\|_{\pi_n},$$

for  $J \in L^2(\pi_n)$ . With  $\hat{E}_n$  we denote the one-sample approximation of  $E_n$ , i.e.  $(\hat{E}_n J)(X_n) = J(X_{n+1})$ , which is better understood in terms of a realization of  $x = (x_0, \dots, x_N)$  of  $X$  as  $(\hat{E}_n J)(x_n) = J(x_{n+1})$ . Moreover,  $\hat{\Pi}_n^K$  is the Monte Carlo approximation of  $\Pi_n^K$ , i.e. if  $x_n^1, \dots, x_n^m$  are i.i.d. samples of  $\pi_n$ , then  $(\hat{\Pi}_n^K J) := \arg \min_{\Phi_K \theta} \frac{1}{m} \sum_{i=1}^m (J(x_n^i) - (\Phi_K \theta)(x_n^i))^2$ . In the following, we write  $\Pi_n$  and  $\hat{\Pi}_n$  whenever  $K$  is fixed.

## 7.2 Theoretical Description of RLSM

We first introduce the *exact algorithm* to compute the continuation value and then give definitions of the 2-step approximation of this exact algorithm. The first step is to introduce projections on the subspace of functions spanned by  $\Phi_K$ , while assuming that (conditional) expectations can be computed exactly. We call this the *idealized algorithm*. We remark that also the projection itself is based on minimizing an expectation. The second step is to introduce Monte Carlo and one-sample approximations of the projections and (conditional) expectations using  $m$  sample paths. This we call the *implementable algorithm*, since it can actually be implemented. Our goal is then to show that the price computed with those two approximation steps converges to the true price, when  $K$  and  $m$  go to  $\infty$ .

### 7.2.1 EXACT ALGORITHMIC

The *continuation value* is the expected discounted payoff at the current time conditioned on a decision not to exercise the option now. The *exact algorithmic* definition of the continuation value is defined backwards step-wise as in (Tsitsiklis and Van Roy, 2001) as

$$\begin{cases} Q_{N-1} & := \alpha E_{N-1} g, \\ Q_n & := \alpha E_n \max(g, Q_{n+1}). \end{cases} \quad (8)$$

### 7.2.2 IDEALIZED ALGORITHM

Our *idealized algorithm* to compute the continuation value, written similar as in (Tsitsiklis and Van Roy, 2001), is defined for fixed  $K$  as

$$\begin{cases} \tilde{Q}_{N-1}^K & := \alpha E_{N-1} P_N^K, \\ \tilde{Q}_n^K & := \alpha E_n P_{n+1}^K, \end{cases} \quad (9)$$

where

$$\begin{cases} P_N^K & := g, \\ P_n^K & := g \mathbf{1}_{g \geq \alpha \Pi_n^K E_n P_{n+1}^K} + \alpha E_n P_{n+1}^K \mathbf{1}_{g < \alpha \Pi_n^K E_n P_{n+1}^K}. \end{cases}$$

In particular,  $P_n^K$  can be interpreted as the choice of the algorithm at time step  $n$ , to either execute and take the payoff or to continue with the expected discounted future payoff. We drop the superscript  $K$  whenever it is clear from the context which  $K$  is meant. We see from this equation, that the difference to the idealized algorithm in (Tsitsiklis and Van Roy, 2001, described in (1) and before Theorem 1) is, that we use the  $\tilde{Q}_{n+1}$  instead of its linear approximation with the random basis functions  $\Pi_n \tilde{Q}_{n+1}$ , if we decide to continue. However, the decision to continue or to stop, is still based on the approximation  $\Pi_n \tilde{Q}_{n+1}$  as it is also the case in the idealized algorithm (Tsitsiklis and Van Roy, 2001). If the linear approximation is exact, both algorithms produce the same output, but if it is not exact, our algorithm uses a better approximation of the continuation value.

### 7.2.3 IMPLEMENTABLE ALGORITHM

Finally, we define our *implementable algorithm* to compute the continuation value, which is an approximation of the idealized algorithm using the approximations  $\hat{E}_n$  and  $\hat{\Pi}_n^K$  as

$$\begin{cases} \hat{Q}_{N-1}^K & := \alpha \hat{E}_{N-1} \hat{P}_N^K, \\ \hat{Q}_n^K & := \alpha \hat{E}_n \hat{P}_{n+1}^K, \end{cases} \quad (10)$$

where

$$\begin{cases} \hat{P}_N^K & := g, \\ \hat{P}_n^K & := g \mathbf{1}_{g \geq \alpha \hat{\Pi}_n^K \hat{E}_n \hat{P}_{n+1}^K} + \alpha \hat{E}_n \hat{P}_{n+1}^K \mathbf{1}_{g < \alpha \hat{\Pi}_n^K \hat{E}_n \hat{P}_{n+1}^K}. \end{cases}$$

Also here we drop the superscript  $K$  whenever it is clear from the context which  $K$  is meant.

### 7.3 Preliminary Results

The following result is similar to the universal approximation theorem of neural networks with random weights (NNRW) proven in (Huang et al., 2006, Theorem II.1). However, while their result is restricted to continuous target functions, we extend it to  $L^2$ -integrable functions. The proof was developed independently.

**Theorem 3.** *Let  $1 \leq n \leq M$  and  $J$  be an integrable function, i.e.  $\|J\|_{\pi_n} < \infty$ , then*

$$\|\Pi_n^K J - J\|_{\pi_n} \xrightarrow[K \rightarrow \infty]{\mathbb{P}\text{-a.s.}} 0.$$

**Lemma 4.** *Let  $\mathcal{X}, \mathcal{Y}$  be a normed spaces and  $\mu$  a probability measure on  $\mathcal{X}$  with the Borel  $\sigma$ -Algebra. Let  $J : \mathcal{X} \times \mathcal{Y} \rightarrow \mathbb{R}$  be a bounded function such that for each  $C > 0$  and each  $x \in \mathcal{X}$  with  $\|x\| < C$  the function  $y \mapsto J(x, y)$  is Lipschitz continuous with Lipschitz constant  $L_C$  (depending only on  $C$  but not on  $x$ ). Then for any  $\epsilon > 0$  and  $y \in \mathcal{Y}$  there exists an open neighbourhood  $O(y, \epsilon) \subset \mathcal{Y}$  such that  $y \in O(y, \epsilon)$  and for every  $\tilde{y} \in O(y, \epsilon)$  we have*

$$\int_{\mathcal{X}} |J(x, y) - J(x, \tilde{y})|^2 d\mu(x) < \epsilon.$$

**Proof** Since  $J$  is bounded, there exists  $M$  such that  $|J| < M$ . Since  $\mu$  is finite, there exists some  $C$  such that  $\mu(\{x \in \mathcal{X} \mid \|x\| \geq C\}) < \frac{\epsilon}{8M^2}$ . Hence, for any  $\tilde{y} \in \mathcal{Y}$

$$\int_{\mathcal{X}} |J(x, y) - J(x, \tilde{y})|^2 \mathbf{1}_{\|x\| \geq C} d\mu(x) < \int_{\mathcal{X}} (2M)^2 \mathbf{1}_{\|x\| \geq C} d\mu(x) < \epsilon/2.$$

Let us choose  $O(y, \epsilon) := B\left(y, \sqrt{\frac{\epsilon}{2L_C^2}}\right)$ , the open ball with radius  $\sqrt{\frac{\epsilon}{2L_C^2}}$  and center  $y$ . Then for any  $x$  with  $\|x\| < C$  and  $\tilde{y} \in O(y, \epsilon)$  we have  $|J(x, y) - J(x, \tilde{y})| < L_C \|y - \tilde{y}\| < \sqrt{\epsilon/2}$ . Therefore,

$$\int_{\mathcal{X}} |J(x, y) - J(x, \tilde{y})|^2 \mathbf{1}_{\|x\| < C} d\mu(x) < \int_{\mathcal{X}} \epsilon/2 d\mu(x) < \epsilon/2.$$

Together, this yields the result. ■

We first prove the following weaker version of the statement of Theorem 3.

**Lemma 5.** *Let  $1 \leq n \leq M$  and  $J$  be an integrable function, i.e.  $\|J\|_{\pi_n} < \infty$ , then*

$$\|\Pi_n^K J - J\|_{\pi_n} \xrightarrow[K \rightarrow \infty]{\tilde{\mathbb{P}}} 0.$$

**Proof** We fix  $\varepsilon > 0$ . We have to show that

$$\lim_{K \rightarrow \infty} \tilde{\mathbb{P}} [\|\Pi_n^K J - J\|_{\pi_n} > \varepsilon] = 0.$$

By the universal approximation theorem (Hornik, 1991, Theorem 1), there exist a 1-hidden layer neural network  $\hat{J}$  with  $n_1$  hidden neurons such that  $\|\hat{J} - J\|_{\pi_n} < \varepsilon/2$ . Without loss of generality we assume that the bias of the last layer is 0, which can be established by introducing another hidden neuron which is constant as function of its input. We notice that also  $\Phi_K \theta$  is a 1-layer neural network with  $K$  hidden nodes (and the same activation function as  $\hat{J}$ ), where the weights of the input layer are i.i.d. sampled of a normal distribution and then fixed and the weights of the output layer are  $\theta$ . Let  $\theta^* \in \mathbb{R}^{n_1}$  be the weights of the output layer of  $\hat{J}$ . For each of the hidden nodes  $1 \leq \nu \leq n_1$  of  $\hat{J}$  we denote the mapping from the input to this hidden node by  $\hat{J}_\nu^h$ . Let  $W_\nu$  be the weights defining  $\hat{J}_\nu^h$ , and denote by  $\Psi$  the operator mapping the weights to the corresponding neural network layer, such that  $\Psi W_\nu = \hat{J}_\nu^h$ . We know from Herrera et al. (2020) that  $\hat{J}_\nu^h$  is Lipschitz continuous w.r.t. the weights for a bounded input  $\|x\| \leq N$ . Moreover, since the activation function is bounded, also  $\hat{J}_\nu^h$  is. Therefore, by Lemma 4 there exists an open neighbourhood  $\mathcal{W}_\nu$  of  $W_\nu$  such that for all  $W \in \mathcal{W}_\nu$  we have

$$\|\Psi W - \Psi W_\nu\|_{\pi_n} < \frac{\varepsilon}{2\sqrt{n_1}|\theta^*|_2}.$$

For any non-empty open set, the probability that a standard Gaussian random variable lies in this open set is positive. Let  $V_k$  be the weights of the  $k$ -th random map  $\phi_k$ , i.e.  $\phi_k = \Psi V_k$  and note that  $V_k$  is a vector of i.i.d. standard Gaussian random variables. Since  $\mathcal{W}_\nu$  is open, we therefore have that  $\tilde{\mathbb{P}}[V_k \in \mathcal{W}_\nu] > 0$ . By independence of the weights we have that with probability 1 each  $\hat{J}_\nu^h$  is approximated well by some  $\phi_k$  when  $K \rightarrow \infty$ . Indeed, let  $K = n_1 \tilde{K}$ , then we have

$$\begin{aligned} \tilde{\mathbb{P}} [\forall 1 \leq \nu \leq n_1 \exists 1 \leq k \leq K : V_k \in \mathcal{W}_\nu] &\geq \tilde{\mathbb{P}} \left[ \forall 1 \leq \nu \leq n_1 \exists (\nu - 1)\tilde{K} < k \leq \nu\tilde{K} : V_k \in \mathcal{W}_\nu \right] \\ &= \prod_{\nu=1}^{n_1} \tilde{\mathbb{P}} \left[ \exists (\nu - 1)\tilde{K} < k \leq \nu\tilde{K} : V_k \in \mathcal{W}_\nu \right] \\ &= \prod_{\nu=1}^{n_1} \left( 1 - \tilde{\mathbb{P}} \left[ \forall (\nu - 1)\tilde{K} < k \leq \nu\tilde{K} : V_k \notin \mathcal{W}_\nu \right] \right) \\ &= \prod_{\nu=1}^{n_1} \left( 1 - \tilde{\mathbb{P}} [V_1 \notin \mathcal{W}_\nu]^{\tilde{K}} \right) \xrightarrow{\tilde{K} \rightarrow \infty} 1, \end{aligned}$$

where we used in line 3 and 5 independence of the weights and for the limit that  $\tilde{\mathbb{P}} [V_1 \notin \mathcal{W}_\nu] < 1$ . We define  $\tilde{\theta}^* \in \mathbb{R}^K$  to have the  $k$ -th coordinate equal to  $\theta_\nu^*$  if  $k = k(\nu) := \arg \min_j \|\phi_j - \hat{J}_\nu^h\|_{\pi_n}$  or 0 otherwise. Here we assume without loss of generality that all  $k(\nu)$  are different (if they are not, the weights are summed up). Then we have

$$\begin{aligned} \|\Pi_n^K J - J\|_{\pi_n} &\leq \|\Phi_K \tilde{\theta}^* - J\|_{\pi_n} \leq \|\Phi_K \tilde{\theta}^* - \hat{J}\|_{\pi_n} + \|\hat{J} - J\|_{\pi_n} \\ &\leq \|\Phi_K \tilde{\theta}^* - \hat{J}\|_{\pi_n} + \varepsilon/2 \end{aligned}$$

and therefore

$$\begin{aligned}\tilde{\mathbb{P}} [\|\Pi_n^K J - J\|_{\pi_n} > \varepsilon] &\leq \tilde{\mathbb{P}} \left[ \|\Phi_K \tilde{\theta}^* - \hat{J}\|_{\pi_n} > \varepsilon/2 \right] \\ &= \tilde{\mathbb{P}} \left[ \|(\Psi V_k)_{k=1}^K \tilde{\theta}^* - (\Psi W_\nu)_{\nu=1}^{n_1} \theta^*\|_{\pi_n} > \varepsilon/2 \right].\end{aligned}$$

Now we notice, that  $\tilde{\theta}_k^*$  is 0 unless  $k = k(\nu)$  for some  $1 \leq \nu \leq n_1$ . Hence,

$$\begin{aligned}\tilde{\mathbb{P}} [\|\Pi_n^K J - J\|_{\pi_n} > \varepsilon] &\leq \tilde{\mathbb{P}} \left[ \|(\Psi V_{k(\nu)})_{\nu=1}^{n_1} \theta^* - (\Psi W_\nu)_{\nu=1}^{n_1} \theta^*\|_{\pi_n} > \varepsilon/2 \right] \\ &\leq \tilde{\mathbb{P}} \left[ \|(\Psi V_{k(\nu)})_{\nu=1}^{n_1} - (\Psi W_\nu)_{\nu=1}^{n_1}\|_{\pi_n} > \frac{\varepsilon}{2|\theta^*|_2} \right] \\ &\leq \tilde{\mathbb{P}} \left[ \exists 1 \leq \nu \leq n_1 : \|\Psi V_{k(\nu)} - \Psi W_\nu\|_{\pi_n} > \frac{\varepsilon}{2\sqrt{n_1}\|\theta^*\|} \right] \\ &= 1 - \tilde{\mathbb{P}} [\forall 1 \leq \nu \leq n_1 \exists 1 \leq k \leq K : V_k \in \mathcal{W}_\nu] \xrightarrow{K \rightarrow \infty} 0.\end{aligned}$$

For the second inequality we used the Cauchy-Schwarz inequality and that  $\|\theta^*\|_{\pi_n} = |\theta^*|_2$ . In the last equality we used that  $k(\nu)$  is chosen such that the distance between  $\Psi V_{k(\nu)}$  and  $\Psi W_\nu$  is minimized.  $\blacksquare$

**Proof** [Theorem 3.] By Lemma 5 we know that  $\|\Pi_n^K J - J\|_{\pi_n} \xrightarrow[K \rightarrow \infty]{\tilde{\mathbb{P}}} 0$  which implies that there exists a subsequence  $(K_m)_{m \geq 1}$  s.t.  $\|\Pi_n^{K_m} J - J\|_{\pi_n} \xrightarrow[m \rightarrow \infty]{\tilde{\mathbb{P}}\text{-a.s.}} 0$ . Let  $\hat{\Omega} \subset \tilde{\Omega}$  with  $\tilde{\mathbb{P}}(\hat{\Omega}) = 1$  be the set on which this convergence holds and let  $\omega \in \hat{\Omega}$ . Hence, for each  $\epsilon > 0$  there exists  $m_\epsilon$  such that for  $m \geq m_\epsilon$  we have  $\|\Pi_n^{K_m} J - J\|_{\pi_n}(\omega) \leq \epsilon$ . Now it is enough to remark that the projection can only get better when more random basis functions are used, since the space on which is projected gets larger, implying that for  $K \leq \tilde{K}$

$$\|\Pi_n^K J - J\|_{\pi_n}(\omega) \geq \|\Pi_n^{\tilde{K}} J - J\|_{\pi_n}(\omega).$$

Therefore, also the original sequence converges at this  $\omega$ , since given  $\epsilon > 0$  for all  $K \geq K_{m_\epsilon}$  we have

$$\|\Pi_n^K J - J\|_{\pi_n}(\omega) \leq \|\Pi_n^{K_{m_\epsilon}} J - J\|_{\pi_n}(\omega) \leq \epsilon.$$

$\blacksquare$

Theorem 3 holds equivalently if neural networks with more than 1 hidden layer are used. The proof is a straight forward extension of the proof given above.

## 7.4 Convergence Results

The price of the Bermudan option approximation of the American option can be expressed with the exact algorithm as

$$U_0 := \max(g(X_0), Q_0(X_0)),$$

the price computed with the idealized algorithm is

$$U_0^K := \max(g(X_0), \tilde{Q}_0^K(X_0))$$

and the price computed with the implementable algorithm is

$$U_0^{K,m} := \max \left( g(X_0), \frac{1}{m} \sum_{i=1}^m \hat{Q}_0^K(x_0, x_1^i, \dots, x_N^i) \right).$$

Combining the following two results, convergence of  $U_0^{K,m_K}$  to  $U_0$  as  $K \rightarrow \infty$  can be established by choosing a suitable sequence  $(m_K)_{K \geq 1}$ .

**Theorem 6.** *The idealized prize  $U_0^K$  converges to the correct price  $U_0$   $\tilde{\mathbb{P}}$ -a.s. as  $K \rightarrow \infty$ .*

**Theorem 7.** *We assume that  $\mathbb{Q}[\alpha \Pi_n^K E_n P_{n+1}^K(X_n) = g(X_n)] = 0$  for all  $0 \leq n \leq N - 1$ . Then the implementable prize  $U_0^{K,m}$  converges almost surely to the idealized price  $U_0^K$  as  $m \rightarrow \infty$ .*

The proofs are a direct consequence of Clément et al. (2001).

**Proof** [Theorems 6 and 7] The proofs are implied by the results presented in (Clément et al., 2001, Section 3). We only need to establish that their assumptions  $A_1$  is satisfied. The assumption  $A_2$  is actually not needed, as explained below.

Assumption  $A_1$  is that  $(\phi_k)_{k \geq 1}$  is total in  $L^2(\sigma(X))$ , which is used to show that  $\|\Pi_n^K Q_n - Q_n\|_{\pi_n}$  converges to 0. We replace this assumption by our Theorem 3, which therefore yields  $\tilde{\mathbb{P}}$ -almost sure convergence in the result.

Assumption  $A_2$  is that for every  $1 \leq n \leq N$  and every  $K > 0$ , if  $\sum_{k=0}^K \lambda_k \phi_k(X_n) = 0$  almost surely, then all  $\lambda_k = 0$ . This assumption is actually only needed for the projection weights to be uniquely defined, such that they can be expressed by the closed-form ordinary least squares formula. Otherwise, if this assumption is not satisfied, there exist several weight vectors  $\theta$ , which all define the same projection  $\Phi_K \theta$  minimizing the projection objective. By Gram-Schmidt we can generate an orthonormal basis  $(\tilde{\phi}_k)_{1 \leq k \leq \tilde{K}(K)}$  of the linear subspace of  $L^2$  that is spanned by  $(\phi_k)_{1 \leq k \leq K}$ , with  $\tilde{K}(K) \leq K$ . By its definition,  $(\tilde{\phi}_k)_{1 \leq k \leq \tilde{K}(K)}$  satisfies assumption  $A_2$  and therefore, the results of (Clément et al., 2001, Section 3) can be applied. Finally, we note that the projections are the same, no matter whether  $(\tilde{\phi}_k)_{1 \leq k \leq \tilde{K}}$  or  $(\phi_k)_{1 \leq k \leq K}$  are used to describe the space that is spanned. We are interested in the convergence of the price. Considering the definition (10), we see that the price depends only on the projection but not on the used weights. Therefore, we can conclude that the same statements hold with our originally defined random basis functions  $(\phi_k)_{1 \leq k \leq K}$ . ■

## 8. Convergence of the Randomized Fitted Q-Iteration (RFQI)

Similar as in Section 7, we first introduce some additional technical notation needed for the proofs. Then we describe the steps from the theoretical idea of RFQI to its implementable version that was presented in Section 3. In contrast to Section 7, the algorithms described here are applied simultaneously for all dates. Again these descriptions are based on (Tsitsiklis and Van Roy, 2001). Finally we prove the main result using Theorem 3 again.

## 8.1 Definitions

In Section 6, Tsitsiklis and Van Roy (2001) introduced a reinforcement learning version of their optimal stopping algorithm, where a stopping function is learned that generalizes over time. In particular, instead of learning a different function for each time step, a single function that gets the time as input is learned with an iterative scheme. In accordance with this, the random basis functions are redefined such that they also take time as input

$$\begin{aligned}\phi_k &: \mathbb{R}^d \times \{0, \dots, N-1\} \rightarrow \mathbb{R}, \\ (x, n) &\mapsto \phi_k(x, n) := \sigma(\alpha_k^\top(x, n)^\top + \beta_k),\end{aligned}$$

with  $\alpha_k \in \mathbb{R}^{d+1}$  and  $\beta_k \in \mathbb{R}$ . For  $0 \leq n \leq N-1$  let  $\Phi_{K,n}$  be defined similar as before as

$$(\Phi_{K,n}\theta)(x) := \theta^\top \phi(x, n) := \sum_{k=1}^K \theta_k \phi_k(x, n),$$

for  $\theta \in \mathbb{R}^K$  and  $x \in \mathbb{R}^d$ . Moreover, let  $\Phi_k := (\Phi_{K,0}, \dots, \Phi_{K,N-1})$ , such that

$$\Phi_k \theta := (\Phi_{K,0}\theta, \dots, \Phi_{K,N-1}\theta).$$

In the following we consider the product space  $(L^2)^N := L^2(\pi_0) \times \dots \times L^2(\pi_{N-1})$ , which is the space on which the functions for all time steps can be defined concurrently. For  $J = (J_0, \dots, J_{N-1}) \in (L^2)^N$  we define the norm

$$\|J\|_\pi := \frac{1}{N} \sum_{n=0}^{N-1} \|J_n\|_{\pi_n},$$

where  $\|\cdot\|_{\pi_n}$  is as defined in Section 7. Let us define the projection operator  $\Pi^K$  as

$$(\Pi^K J) := \arg \min_{\Phi_K \theta} \|\Phi_K \theta - J\|_\pi,$$

for  $J = (J_0, \dots, J_{N-1}) \in (L^2)^N$ . Finally we define the operator

$$H : (L^2)^N \rightarrow (L^2)^N, \quad \begin{pmatrix} J_0 \\ \vdots \\ J_{N-2} \\ J_{N-1} \end{pmatrix} \mapsto \begin{pmatrix} \alpha E_0 \max(g, J_1) \\ \vdots \\ \alpha E_{N-2} \max(g, J_{N-1}) \\ \alpha E_{N-1} g \end{pmatrix}, \quad (11)$$

where  $E_n$  and  $g$  are as defined in the previous sections.

## 8.2 Theoretical Description of the Algorithm

Based on the definitions in Section 7.2, we first introduce the *exact algorithm* and then give the 2-step approximation with the *idealized* and *implementable algorithm*.

### 8.2.1 EXACT ALGORITHM

Let  $Q_n$  as defined in (8), then  $Q := (Q_0, \dots, Q_{N-1})$  satisfies  $Q = HQ$  by definition. In particular,  $Q$  is a fixed-point of  $H$ . It was shown in (Tsitsiklis and Van Roy, 2001, Section 6) that  $H$  is a contraction with respect to the norm  $\|\cdot\|_\pi$  with contraction factor  $\alpha$ . Hence, the Banach fixed-point theorem implies that there exists a unique fixed-point, which therefore has to be  $Q$ , and that for any starting element  $J^0 \in (L^2)^N$ ,  $J^i$  converges to  $Q$  in  $(L^2)^N$  as  $i \rightarrow \infty$ , where  $J^{i+1} := HJ^i$ . This yields a way to find the *exact algorithm*  $Q$  iteratively.

### 8.2.2 IDEALIZED ALGORITHM

The combined operator  $\Pi^K H$  is a contraction on the space  $\Pi^K(L^2)^N$ , since the projection operator is a non-expansion as outlined in (Tsitsiklis and Van Roy, 2001, Section 6). The *idealized algorithm* is then defined as the unique fixed-point  $\tilde{Q}^K$  of  $\Pi^K H$ , which can again be found by iteratively applying this operator to some starting element. Since any element in  $\Pi^K(L^2)^N$  is given as  $\Phi_K \theta$  for some weight vector  $\theta \in \mathbb{R}^K$ , this iteration can equivalently be given as iteration on the weight vectors. To do this, let us assume without loss of generality that  $(\phi_k)_{1 \leq k \leq K}$  are independent (if not, see the strategy in Proof of Theorem 6 and 7). Then, given some starting weight vector  $\theta_K^0$ , the iterative application of  $\Pi^K H$  defines the weight vectors

$$\theta_K^{i+1} := \alpha \left( \mathbb{E} \left[ \sum_{n=0}^{N-1} \phi_{1:K}^\top(X_n, n) \phi_{1:K}(X_n, n) \right] \right)^{-1} \cdot \mathbb{E} \left[ \sum_{n=0}^{N-1} \phi_{1:K}^\top(X_n, n) \cdot \max(g(X_{n+1}), (\Phi_{K,n+1} \theta_K^i)(X_{n+1})) \right],$$

where  $\phi_{1:K} = (\phi_1, \dots, \phi_K)$ . This closed-form solution is exactly the ordinary least squares (OLS) formula and this result was shown in (Tsitsiklis and Van Roy, 2001, Section 6).

### 8.2.3 IMPLEMENTABLE ALGORITHM

An *implementable version* of this iteration is defined by the Monte Carlo approximation of the weight vectors. In particular, we assume that  $m$  realizations  $(x_0^j, \dots, x_N^j)_{1 \leq j \leq m}$  of  $X$  are sampled and fixed for all iterations. Then for  $\hat{\theta}_{K,m}^0 = \theta_K^0$  we iteratively define

$$\hat{\theta}_{K,m}^{i+1} := \alpha \left( \sum_{j=1}^m \sum_{n=0}^{N-1} \phi_{1:K}^\top(x_n^j, n) \phi_{1:K}(x_n^j, n) \right)^{-1} \cdot \sum_{j=1}^m \sum_{n=0}^{N-1} \phi_{1:K}^\top(x_n^j, n) \cdot \max(g(x_{n+1}^j), (\Phi_{K,n+1} \hat{\theta}_{K,m}^i)(x_{n+1}^j)),$$

which in turn define  $\hat{Q}^{K,m,i} := \Phi_K \hat{\theta}_{K,m}^i$ . As explained in (Tsitsiklis and Van Roy, 2001, Section 6), this implementable iteration can equivalently be described as iteratively applying the operator  $\widehat{\Pi^K H}$ . Here  $\widehat{\Pi^K H}$  is identical to  $\Pi^K H$ , but with the measures  $\pi_n$  replaced by the empirical measures  $\hat{\pi}_n$  arising from the sampled trajectories  $(x_0^j, \dots, x_N^j)_{1 \leq j \leq m}$ . Hence,

$\widehat{\Pi^K H}$  is also a contraction and Banach's fixed-point theorem implies convergence to the unique fixed point

$$\hat{Q}^{K,m,i} \xrightarrow{i \rightarrow \infty} \hat{Q}^{K,m} =: \Phi_K \hat{\theta}_{K,m}^*.$$

We note that this also implies that  $\hat{\theta}_{K,m}^i \xrightarrow{i \rightarrow \infty} \hat{\theta}_{K,m}^*$ .

### 8.3 Convergence Result

In the following we show that prices of Bermudan options computed with the two approximation steps of the exact algorithm converge to the correct price, as  $K$  and  $m$  go to  $\infty$ . The prices are defined similar as in Section 7.4. Hence, it is enough to show that  $\hat{Q}^{K,m,i}$  converges to  $\tilde{Q}^K$  as  $i \rightarrow \infty$  and that  $\tilde{Q}^K$  converges to  $Q$  as  $K \rightarrow \infty$ .

**Theorem 8.**  $\tilde{Q}^K$  converges  $\tilde{\mathbb{P}}$ -a.s. to  $Q$  as  $K \rightarrow \infty$ , i.e.

$$\|\tilde{Q}^K - Q\|_\pi \xrightarrow[K \rightarrow \infty]{\tilde{\mathbb{P}}\text{-a.s.}} 0.$$

**Proof** First, let us recall (Tsitsiklis and Van Roy, 2001, Theorem 3), which states that for  $0 < \kappa < 1$  the contraction factor of  $\Pi^K H$ , we have

$$\|\tilde{Q}^K - Q\|_\pi \leq \frac{1}{\sqrt{1 - \kappa^2}} \|\Pi^K Q - Q\|_\pi.$$

Now remark that since  $\Pi^K$  is a non-expansion and  $H$  a contraction with factor  $\alpha$ , we have  $\kappa \leq \alpha < 1$ . Therefore, for every  $K$  we have

$$\|\tilde{Q}^K - Q\|_\pi \leq \frac{1}{\sqrt{1 - \alpha^2}} \|\Pi^K Q - Q\|_\pi. \quad (12)$$

Finally, we remark that Theorem 3 holds equivalently for the norm  $\|\cdot\|_\pi$ , since the universal approximation theorem can equivalently be applied for functions with the combined input  $(x, n)$ . Hence, the right hand side of (12) converges to 0  $\tilde{\mathbb{P}}$ -a.s. as  $K \rightarrow \infty$ .  $\blacksquare$

We recall that the weight vectors  $\hat{\theta}_{K,m}^i$  are random variables since they depend on the  $m$  sampled trajectories of  $X$ .

**Lemma 9.** For any fixed  $i \in \mathbb{N}$  we have that  $\hat{\theta}_{K,m}^i$  converges to  $\theta_K^i$   $\mathbb{Q}$ -a.s. as  $m \rightarrow \infty$ .

**Proof** The proof follows the proof of (Tsitsiklis and Van Roy, 2001, Theorem 2) We introduce the intermediate weight as

$$\begin{aligned} \tilde{\theta}_{K,m}^i := & \alpha \left( \sum_{j=1}^m \sum_{n=0}^{N-1} \phi_{1:K}^\top(x_n^j, n) \phi_{1:K}(x_n^j, n) \right)^{-1} \\ & \cdot \sum_{j=1}^m \sum_{n=0}^{N-1} \phi_{1:K}^\top(x_n^j, n) \cdot \max \left( g(x_{n+1}^j), (\Phi_{K,n+1} \theta_K^{i-1})(x_{n+1}^j) \right). \end{aligned}$$

Then it is clear that  $\tilde{\theta}_{K,m}^i$  converges to  $\theta_K^i$   $\mathbb{Q}$ -a.s. as  $m \rightarrow \infty$ , by the strong law of large numbers. Hence,  $\delta_i(m) := |\tilde{\theta}_{K,m}^i - \theta_K^i|_2$  converges to 0  $\mathbb{Q}$ -a.s. Moreover, for suitably chosen random variables  $A_i(m)$  that remain bounded as  $m \rightarrow \infty$ , we have

$$\hat{\theta}_{K,m}^i - \tilde{\theta}_{K,m}^i = A_i(m) |\hat{\theta}_{K,m}^{i-1} - \theta_K^{i-1}|_2.$$

Therefore we have by the triangle inequality

$$|\hat{\theta}_{K,m}^i - \theta_K^i|_2 \leq \delta_i(m) + A_i(m) |\hat{\theta}_{K,m}^{i-1} - \theta_K^{i-1}|_2.$$

Since (by our choice) we start with the same weight vector  $\hat{\theta}_{K,m}^0 = \theta_K^0$ , we can conclude by induction that

$$|\hat{\theta}_{K,m}^i - \theta_K^i|_2 \xrightarrow[m \rightarrow \infty]{\mathbb{Q}\text{-a.s.}} 0.$$

However, we remark that this proof only works as long as  $i$  is fixed, but not in the limit  $i \rightarrow \infty$ , since there induction would lead to an infinity sum.  $\blacksquare$

**Theorem 10.** *Let  $K \in \mathbb{N}$  be fixed. Then there exists a random sequence  $(m_i)_{i \geq 0}$  such that  $\hat{Q}^{K,m_i,i}$  converges  $\mathbb{Q}$ -a.s. to  $\tilde{Q}^K$  as  $i \rightarrow \infty$ , i.e.*

$$\|\hat{Q}^{K,m_i,i} - \tilde{Q}^K\|_\pi \xrightarrow[i \rightarrow \infty]{\mathbb{Q}\text{-a.s.}} 0.$$

**Proof** Let us define  $\theta_K^* \in \mathbb{R}^K$  to be weight vector of the unique fixed-point  $\tilde{Q}^K$  of  $\Pi^K H$ , i.e.  $\tilde{Q}^K = \Phi_K \theta_K^*$ . From Banach's fixed-point theorem we know that  $|\theta_K^i - \theta_K^*|_2 \rightarrow 0$  as  $i \rightarrow \infty$ . With Lemma 9 we know that for every  $i \in \mathbb{N}$  there exists  $\Omega_i \subset \Omega$  with  $\mathbb{Q}(\Omega_i) = 1$  such that  $\hat{\theta}_{K,m}^i(\omega)$  converges to  $\theta_K^i$  for all  $\omega \in \Omega_i$ . Let  $\Omega_\infty := \cap_{i=1}^\infty \Omega_i$  be the set on which this convergence holds for all  $i \in \mathbb{N}$ , then  $\mathbb{Q}(\Omega_\infty) = 1$ . Fix  $\omega \in \Omega_\infty$ . Now let us choose  $m_0 = 0$  and for every  $i > 0$ ,  $m_i > m_{i-1}$  such that  $|\hat{\theta}_{K,m_i}^i(\omega) - \theta_K^i|_2 \leq 1/i$ . Therefore, we obtain that

$$|\hat{\theta}_{K,m_i}^i(\omega) - \theta_K^*|_2 \leq |\hat{\theta}_{K,m_i}^i(\omega) - \theta_K^i|_2 + |\theta_K^i - \theta_K^*|_2 \leq \frac{1}{i} + |\theta_K^i - \theta_K^*|_2,$$

which converges to 0 when  $i$  tends to infinity.  $\blacksquare$

## 9. Conclusion

Based on a broad study of machine learning based approaches to approximate the solution of optimal stopping problems, we introduced two simple and powerful approaches, RLSM and RFQI. They have the advantage of the state-of-the-art; they are very simple to implement and have convergence guarantees. Moreover, they have the advantages of neural networks; they are easily scalable to high dimensions, and there is no need to choose basis functions by hand. On top of that, these methods are extremely fast. In Markovian problems, RFQI outperforms all existing methods reconfirming that reinforcement learning methods surpass backward induction methods. In non-Markovian problems, our randomized recurrent neural network

algorithm RRLSM, achieves similar results as the path-version of DOS, while using less training data and being much faster. However, this problem also brought up the limitations of reinforcement learning approaches, which do not work well outside Markovian settings. The speed of our algorithms is very promising for applications in high dimensions and with many discretization dates, where existing methods might become impractical.

## Acknowledgments

The authors would like to thank Hartmut Maennel and Louis Paulot for helpful feedback and discussions. Moreover, the authors would like to acknowledge support for this project from the Swiss National Science Foundation (SNF grant 179114).

## References

- Eduardo Abi Jaber and Omar El Euch. Multifactor approximation of rough volatility models. *SIAM Journal on Financial Mathematics*, 10(2):309–349, 2019.
- Leif Andersen. A simple approach to the pricing of bermudan swaptions in the multi-factor libor market model. volume 3, pages 5–32, 1999.
- Vlad Bally and Gilles Pagès. A quantization algorithm for solving multi-dimensional discrete-time optimal stopping problems. *Bernoulli*, 9(6):1003–1049, 2003.
- Vlad Bally, Gilles Pagès, and Jacques Printems. A quantization tree method for pricing and hedging multidimensional american options. *Mathematical Finance*, 15(1):119–168, 2005.
- Jérôme Barraquand and Didier Martineau. Numerical valuation of high dimensional multivariate american securities. *The Journal of Financial and Quantitative Analysis*, 30(3):383–405, 1995.
- Christian Bayer, Peter Friz, and Jim Gatheral. Pricing under rough volatility. *Quantitative Finance*, 16(6):887–904, 2016.
- Sebastian Becker, Patrick Cheridito, and Arnulf Jentzen. Deep optimal stopping. *Journal of Machine Learning Research*, 20:74, 2019.
- Sebastian Becker, Patrick Cheridito, and Arnulf Jentzen. Pricing and hedging american-style options with deep learning. *Journal of Risk and Financial Management*, 2020.
- Dimitri P. Bertsekas and John N. Tsitsiklis. *Neuro-Dynamic Programming*. Athena Scientific, 1996.
- Bruno Bouchard and Xavier Warin. Monte-carlo valuation of american options: Facts and new algorithms to improve existing methods. pages 215–255, 2012.
- Phelim P. Boyle, Adam W. Kolkiewicz, and Ken Seng Tan. An improved simulation method for pricing high-dimensional american derivatives. *Mathematics and Computers in Simulation*, 62(3):315 – 322, 2003.

- Steven J. Bradtke and Andrew G. Barto. Linear least-squares algorithms for temporal difference learning. *Machine learning*, 1996.
- Mark Broadie and Paul Glasserman. A stochastic mesh method for pricing high-dimensional american options. *Journal of Computational Finance*, 7(4):35–72, 2004.
- Weipeng Cao, Xizhao Wang, Zhong Ming, and Jinzhu Gao. A review on neural networks with random weights. *Neurocomputing*, 275:278 – 287, 2018.
- Jacques F. Carriere. Valuation of the early-exercise price for options using simulations and nonparametric regression. *Insurance: Mathematics and Economics*, 19(1):19 – 30, 1996.
- Shuhang Chen, Adithya M Devraj, Ana Bušić, and Sean Meyn. Zap q-learning for optimal stopping. *IEEE American Control Conference (ACC)*, pages 3920–3925, 2020.
- Emmanuelle Clément, Damien Lamberton, and Philip Protter. An analysis of the longstaff-schwartz algorithm for american option pricing. Technical report, Cornell University Operations Research and Industrial Engineering, 2001.
- Daniel Egloff, Michael Kohler, and Nebojsa Todorovic. A dynamic look-ahead monte carlo algorithm for pricing bermudan options. *The Annals of Applied Probability*, 17(4): 1138–1171, 2007.
- Omar El Euch, Masaaki Fukasawa, and Mathieu Rosenbaum. The microstructural foundations of leverage effect and rough volatility. *Finance and Stochastics*, 22(2):241–280, 2018.
- Claudio Gallicchio, Alessio Micheli, and Luca Pedrelli. Deep reservoir computing: A critical experimental analysis. *Neurocomputing*, 268:87 – 99, 2017.
- Diego Garcia. Convergence and biases of monte carlo estimates of american option prices using a parametric exercise rule. *Journal of Economic Dynamics and Control*, 27(10):1855 – 1879, 2003.
- Jim Gatheral, Thibault Jaisson, and Mathieu Rosenbaum. Volatility is rough. *Quantitative Finance*, 18(6):933–949, 2018.
- Alexander N. Gorban, Ivan Yu. Tyukin, Danil V. Prokhorov, and Konstantin I. Sofeikov. Approximation with random bases: Pro et contra. *Information Sciences*, 364-365:129–145, 2016.
- Hamza Hanbali and Daniel Linders. American-type basket option pricing: a simple two-dimensional partial differential equation. *Quantitative Finance*, 19(10):1689–1704, 2019.
- Martin B. Haugh and Leonid Kogan. Pricing american options: A duality approach. *Operations Research*, 52(2):258–270, 2004.
- Calypso Herrera, Florian Krach, and Josef Teichmann. Estimating full lipschitz constants of deep neural networks. *arXiv:2004.13135*, 2020.

- Steven L. Heston. A closed-form solution for options with stochastic volatility with applications to bond and currency options. *The review of financial studies*, 6(2):327–343, 1993.
- Kurt Hornik. Approximation capabilities of multilayer feedforward networks. *Neural networks*, 4(2):251–257, 1991.
- Guang-Bin Huang, Lei Chen, Chee Kheong Siew, et al. Universal approximation using incremental constructive feedforward networks with random hidden nodes. *IEEE Transactions on Neural Networks*, 17(4):879–892, 2006.
- Shashi Jain and Cornelis W. Oosterlee. The stochastic grid bundling method: Efficient pricing of bermudan options and their greeks. *Applied Mathematics and Computation*, 269: 412 – 431, 2015.
- Leslie Pack Kaelbling, Michael L. Littman, and Andrew W. Moore. Reinforcement learning: A survey. *Journal of artificial intelligence research*, 4:237–285, 1996.
- Michael Kohler, Adam Krzyżak, and N Zaklina Todorovic. Pricing of high-dimensional american options by neural networks. *Wiley-Blackwell: Mathematical Finance*, 2010.
- Anastasia Kolodko and John Schoenmakers. Iterative construction of the optimal bermudan stopping time. *Finance and Stochastic*, 10:27–49, 2004.
- Bernard Lapeyre and Jérôme Lelong. Neural network regression for bermudan option pricing, 2019.
- Yuxi Li, Csaba Szepesvari, and Dale Schuurmans. Learning exercise policies for american options. In *International Conference on Artificial Intelligence and Statistics*, 2009.
- Giulia Livieri, Saad Mouti, Andrea Pallavicini, and Mathieu Rosenbaum. Rough volatility: evidence from option prices. *IISE transactions*, 50(9):767–776, 2018.
- Francis A. Longstaff and Eduardo S. Schwartz. Valuing american options by simulation: a simple least-squares approach. *Review of Financial Studies*, 2001.
- Mantas Lukoševičius and Herbert Jaeger. Reservoir computing approaches to recurrent neural network training. *Computer Science Review*, 3(3):127 – 149, 2009.
- Gilles Pagès. *Numerical Probability: An Introduction with Applications to Finance*. Springer, 2018.
- Chris Rogers. Monte carlo valuation of american options. *Mathematical Finance*, 12(3): 271–286, 2002.
- Chris Rogers. Dual valuation and hedging of bermudan options. *SIAM Journal on Financial Mathematics*, 1(1):604–608, 2010.
- Benjamin Schrauwen, David Verstraeten, and Jan Van Campenhout. An overview of reservoir computing: theory, applications and implementations. In *European Symposium on Artificial Neural Networks*, pages 471–482, 2007.

- Richard S. Sutton and Andrew G. Barto. *Reinforcement Learning: An Introduction*. 2018.
- James A. Tilley. Valuing american options in a path simulation model. 1993.
- John Tsitsiklis and Benjamin Van Roy. Optimal stopping of markov processes: Hilbert space theory, approximation algorithms, and an application to pricing high-dimensional financial derivatives. *IEEE Transactions on Automatic Control*, 44:1840–1851, 1997.
- John Tsitsiklis and Benjamin Van Roy. Regression methods for pricing complex american-style options. *IEEE Transactions on Neural Networks*, 12(4):694–703, 2001.
- David Verstraeten, Benjamin Schrauwen, Michiel d’Haene, and Dirk Stroobandt. An experimental unification of reservoir computing methods. *Neural Networks*, 20(3):391 – 403, 2007. Echo State Networks and Liquid State Machines.
- Huizhen Yu and Dimitri P. Bertsekas. Q-learning algorithms for optimal stopping based on least squares. *European Control Conference*, 2007.